Journal of Volcanology and Geothermal Research 189 (2010) 57–80

Contents lists available at ScienceDirect

Journal of Volcanology and Geothermal Research

journal homepage: www.elsevier.com/locate/jvolgeores

Large-volume silicic volcanism in Kamchatka: Ar–Ar and U–Pb ages, isotopic, and geochemical characteristics of major pre-Holocene caldera-forming eruptions

I.N. Bindeman [a,*], V.L. Leonov [b], P.E. Izbekov [c], V.V. Ponomareva [b], K.E. Watts [a], N.K. Shipley [a], A.B. Perepelov [d], L.I. Bazanova [b], B.R. Jicha [e], B.S. Singer [e], A.K. Schmitt [f], M.V. Portnyagin [g], C.H. Chen [h]

[a] Geological Sciences, 1272 University of Oregon, Eugene, OR 97403, USA
[b] Institute of Volcanology and Seismology, Petropavlovsk-Kamchatsky, Russia
[c] Geophysical Institute, University of Alaska, Fairbanks, AK, USA
[d] Vinogradov Institute of Geochemistry, Irkutsk, Russia
[e] Geology and Geophysics, University of Wisconsin, Madison, WI, USA
[f] Earth and Space Sciences, UCLA, Los Angeles, CA, USA
[g] Leibnitz Institute for Marine Sciences, IfM-GEOMAR, Kiel, Germany
[h] Institute of Earth Sciences, Academia Sinica, P.O. Box 1-55 Nankang, Taipei 11529, Taiwan

ARTICLE INFO

Article history:
Received 9 March 2009
Accepted 20 October 2009
Available online 3 November 2009

Keywords:
Kamchatka
calderas
zircon
geochronology
climate change
Ar–Ar
oxygen isotopes

ABSTRACT

The Kamchatka Peninsula in far eastern Russia represents the most volcanically active arc in the world in terms of magma production and the number of explosive eruptions. We investigate large-scale silicic volcanism in the past several million years and present new geochronologic results from major ignimbrite sheets exposed in Kamchatka. These ignimbrites are found in the vicinity of morphologically-preserved rims of partially eroded source calderas with diameters from ~2 to ~30 km and with estimated volumes of eruptions ranging from 10 to several hundred cubic kilometers of magma. We also identify and date two of the largest ignimbrites: Golygin Ignimbrite in southern Kamchatka (0.45 Ma), and Karymshina River Ignimbrites (1.78 Ma) in south-central Kamchatka. We present whole-rock geochemical analyses that can be used to correlate ignimbrites laterally. These large-volume ignimbrites sample a significant proportion of remelted Kamchatkan crust as constrained by the oxygen isotopes. Oxygen isotope analyses of minerals and matrix span a 3‰ range with a significant proportion of moderately low-δ^{18}O values. This suggests that the source for these ignimbrites involved a hydrothermally-altered shallow crust, while participation of the Cretaceous siliceous basement is also evidenced by moderately elevated δ^{18}O and Sr isotopes and xenocryst contamination in two volcanoes. The majority of dates obtained for caldera-forming eruptions coincide with glacial stages in accordance with the sediment record in the NW Pacific, suggesting an increase in explosive volcanic activity since the onset of the last glaciation 2.6 Ma. Rapid changes in ice volume during glacial times and the resulting fluctuation of glacial loading/unloading could have caused volatile saturation in shallow magma chambers and, in combination with availability of low-δ^{18}O glacial meltwaters, increased the proportion of explosive vs effusive eruptions. The presented results provide new constraints on Pliocene–Pleistocene volcanic activity in Kamchatka, and thus constrain an important component of the Pacific Ring of Fire.

1. Introduction

The Kamchatka Peninsula in far eastern Russia (Fig. 1) is one of the most active arc segments on Earth (Simkin and Siebert, 1994), with the largest number of collapse calderas per unit of arc length (Hughes and Mahood, 2008) and high magma and volatile output rates (Portnyagin et al., 2007; Taran, 2009). Built on accreted ocean arc terrains and slivers of Asian continental crust (Geist et al., 1994; Konstantinovskaia, 2001; Bindeman et al., 2002; Lander and Shapiro, 2007), it has been volcanically active for more than 70 Ma as a result of a nearly head on collision of the Kula and Pacific Plates with the Asian mainland (Fig. 1). Since the Late Eocene volcanic front was located in the accreted terrain of the Sredinny Range. Accretion of the Eastern Kamchatka Intraoceanic Terrain and the Pliocene accretion of cape-peninsulas onto Eastern Kamchatka (e.g., Lander and Shapiro, 2007) resulted in locking of the subduction zone, breaking-off and sinking of the subducting Kula Plate, and the subsequent subduction zone migrating east, to its present location. This transition initiated the formation of the Eastern Volcanic Front and the volcanic zone of the Central Kamchatka Depression, while activity on the former volcanic front in the Sredinny Range diminished.

Volcanism patterns reflect Kamchatka's tectonic history from the Eocene to the present (e.g., Avdeiko et al., 2007) and are expressed in

* Corresponding author. Tel.: +1 541 346 3817.
E-mail address: bindeman@uoregon.edu (I.N. Bindeman).

0377-0273/$ – see front matter © 2009 Elsevier B.V. All rights reserved.
doi:10.1016/j.jvolgeores.2009.10.009

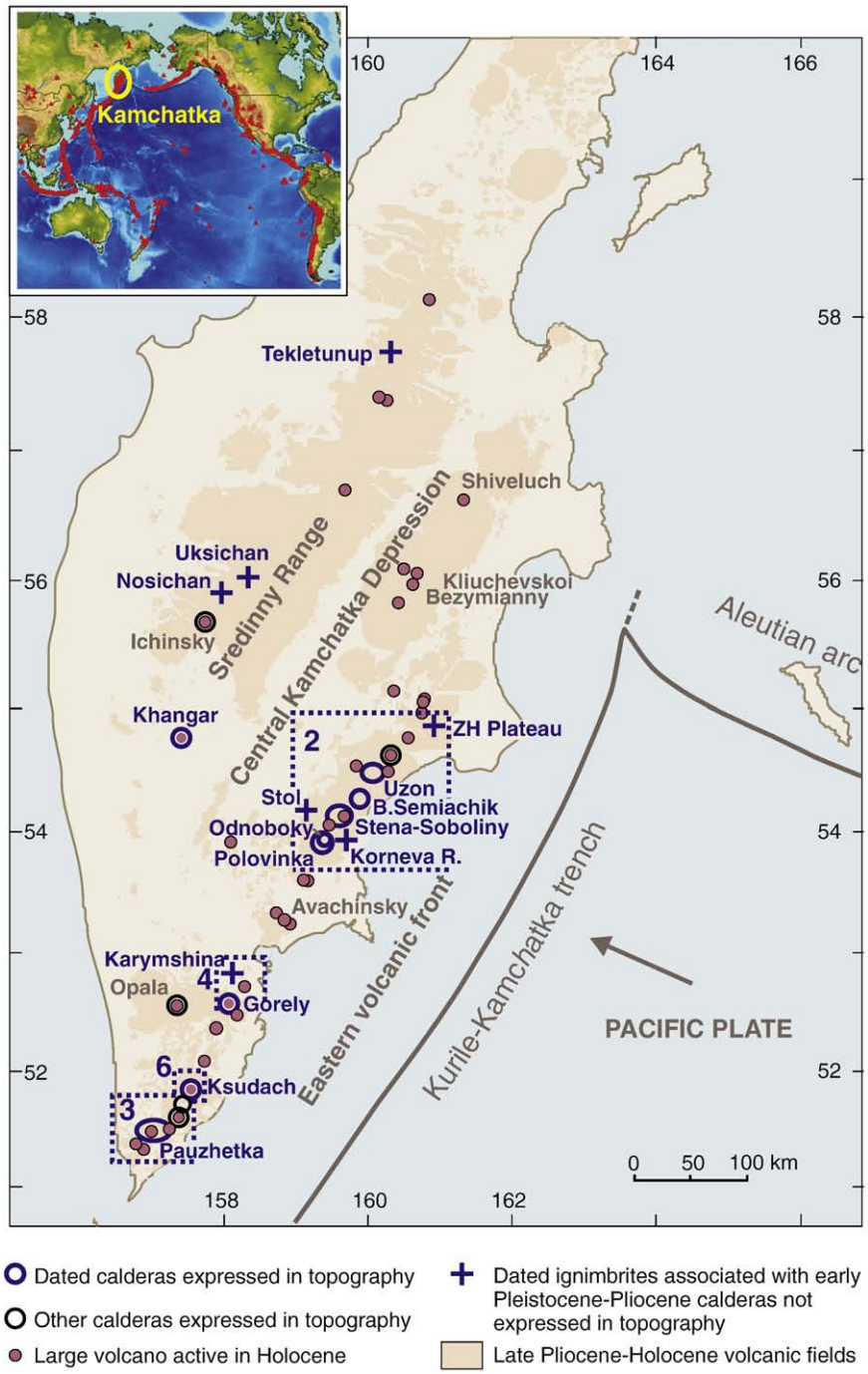

Fig. 1. Dated calderas and ignimbrites in Kamchatka. Numbered frames indicate areas shown in Figs. 2–5.

three main volcanic belts (Fig. 1); the Sredinny Range, the Eastern Volcanic Front (EVF), and the Central Kamchatka Depression (CKD). In the CKD, the voluminous basaltic-intermediate volcanoes (Kliuchevskoi, Shiveluch, Bezymyanny) are the most active in the world. The majority of the calderas in Kamchatka occur in the Sredinny Range and the EVF (Fig. 1) and are associated with areas of long-term magmatism. The investigation of calderas in Kamchatka spans more than 40 years (Erlich et al., 1972; Erlich, 1986; Fedotov and Masurenkov, 1991; Leonov and Grib, 2004), but the majority of work has been published in Russian and remains relatively unknown in international literature. Furthermore, poor geological exposure and insufficient prior dating efforts resulted in interpretations that many collapse calderas were "volcano–tectonic depressions", negative volcanic forms that develop over several hundred thousand years through a combination of volcanic activity, tectonic downdrop, and glacial erosion. Although the level of investigation of Holocene post-glacial explosive eruptions, including correlation of their tephra, is superb and arguably one of the best in the world (Braitseva et al., 1987, 1995, 1997; Gusev et al., 2003; Ponomareva et al., 2004, 2007a,b), several factors prevent investigation of Pleistocene and older calderas: poor geological exposure, high uplift and erosion rates, tectonic burial rates, high volcanic activity that leads to concealing old volcanic products, heavy vegetation cover, and poor road infrastructure. For the same reasons, eruptive volume estimates for Kamchatkan calderas are imprecise. A rough correlation of caldera sizes, and thicknesses of outflow ignimbrite sheets all suggest eruption volumes in excess of 100 km^3, and possibly >400 km^3 for some calderas (e.g., Karymshina and Pauzhetka, see below).

As a result of decades-long efforts in geological mapping, and identification of most thick ignimbrites sheets in Kamchatka, our knowledge on calderas is much more complete (Erlich et al., 1972; Melekestsev et al., 1974; Melekestsev, 1980; Erlich, 1986; Leonov and Grib, 2004). In most cases, outcrops of these ignimbrites are located near topographically exposed calderas and caldera clusters visible on air photos or space images (Fig. 2). In many cases the source caldera is identified for an ignimbrite sheet based on geological correlation, mineralogy (e.g. ± quartz or biotite) and major element composition of eruptive products (e.g. Grib and Leonov, 1993a,b). However, there is a lack of knowledge regarding the number of eruptions per each center and their associated volumes within caldera complexes.

Compositionally, Kamchatkan caldera-forming ignimbrites have clear distinctions in K_2O and SiO_2 contents and inherited their chemistry from their parental basaltic magmas and/or their crustal source regions (Fig. 9c). Given that all volcanic rocks in the Kurile–Kamchatka Volcanic Arc exhibit strong across-arc geochemical zonation that results in a ten-fold increase in K_2O across the arc (Volynets, 1994; Churikova et al., 2001; Duggen et al., 2007), magmas in the Sredinny Range are most K_2O-rich and contain biotite, while the majority of EVF rocks are K_2O-poorer. Oxygen isotopic variations in Kamchatkan silicic rocks were shown to be large, spanning 3‰ (Bindeman et al., 2004), with a particularly large abundance of low-$\delta^{18}O$ values (Fig. 9a,b). This result was interpreted to stem from the influence of the last glaciation: low-$\delta^{18}O$ glacial meltwaters imprinted their isotopic signature on hydrothermally-altered rocks that contributed to the crustal magmas through remelting and assimilation. Sr isotopic values of Kamchatkan rocks span 0.703–0.706, with higher values characteristic for the Sredinny Range Magmas (Pokrovsky and Volynets, 1999; Dril et al., 1999; Bindeman et al., 2004).

Investigation of the influence of the last glaciation on explosive volcanic activity in Kamchatka deserves consideration because glacial retreats and advances could have contributed to the periodicity of the largest explosive volcanic eruptions, and below we attempt to find a correlation between them. Contrary to the idea that glacial overload increases repose interval (Wallman et al., 1988), and deglaciation increases mantle melting (Slater et al., 1998), examination of the deep sea ash record suggests increased explosivity in Kamchatka during Late Quaternary glaciations. Several ODP holes (882, 883, 884 and others) were drilled near Kamchatka's coasts and sediment cores spanning the last several million years were retrieved from them. Prueher and Rea (2001a,b) and Cao et al. (1995) have examined the number and thickness of ash layers in these cores and discovered that the onset of the Northern Hemisphere glaciation in Kamchatka at 2.6 Ma coincided with a sharp increase of explosive volcanism, as revealed by abundant ice rafted debris in the sedimentary record, (also noted by Bigg et al., 2008). Correlation of thicknesses of ash deposits, in combination with examination of their whole-rock and glass-shard chemistry (e.g., Cao et al., 1995) helps to identify the time intervals of increased explosive activity (and their relation to glacial–interglacial periods), and, in the case of several thicker ash layers that occur in the core, specific large-volume eruptions. Thus, a combined effort that includes dating and compositional fingerprinting of major subaerial ignimbrite sheets and correlation with their marine ash layer equivalents based on sedimentary stratigraphic age and composition serves several purposes.

This work reports Ar–Ar and U–Pb zircon ages of major ignimbrite eruptions in Kamchatka over the past several million years and their compositional (major and trace element), and isotopic values. Thus this work expands on the number of defined calderas in the existing databases (e.g. Geyer and Marti, 2008, Cambridge University database, Hughes and Mahood, 2008) and provides expanded and refined

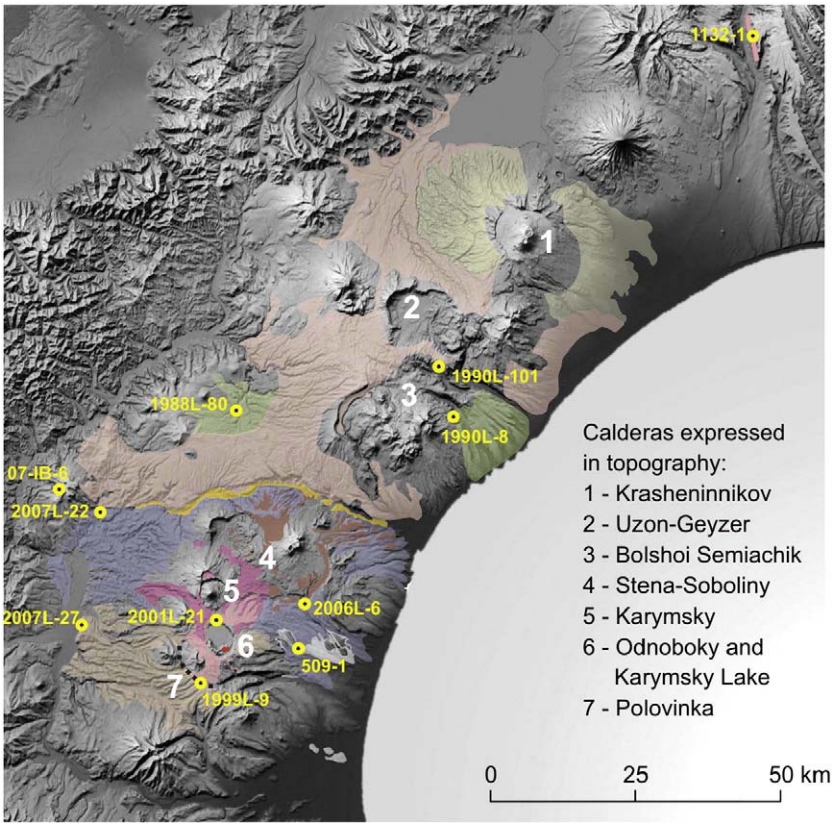

Fig. 2. Calderas and associated ignimbrites of the central part of Eastern Kamchatka. Location of this area is shown by Frame 2 in Fig. 1. Ignimbrite sheets associated with the individual caldera complexes are shown with different colors; their outlines are based on the maps of Masurenkov (1980), Florensky and Trifonov (1985), Leonov and Grib (2004). Location of the dated samples is shown with yellow circles. Some ignimbrite sheets are covered by younger sediments and are exposed only in river banks. See Table 1 for ages and text for details. Uzon, Polovinka and Stena–Soboliny ignimbrites are multi-stage sheets and may represent a suite of repetitive eruptions from these eruptive centers. Distribution of the individual ignimbite sheets somewhat differs when mapped by different researchers and requires further refining.

Table 1
Major caldera-forming eruptions of Kamchatka, their sizes, ages and oxygen isotopic characteristics of eruptive products. 1 — IN Bindeman; 2 — VL Leonov; 3 — AA Perepelov; 4 — LI Bazanova; 5 — EN Grib; 6 — PE Izbekov, and 7 IV Melekestsev. Reference: 11 — Ponomareva et al. (2004); 12 — Selyangin and Ponomareva, 1999; Leonov and Grib, 2004; 14 — Masurenkov, 1980; and 15 — Braitseva et al. (1996). Braitseva et al. (1995); SiO2 and $\delta^{18}O$ values for Late Pleistocene–Holocene caldera samples are from Bindeman et al. (2004).

Caldera or ignimbrite	Sample	Material	Caldera size (km)	Thickness of proximal ignimbrite	Estimated eruptive vol	Mineral dated	Ar–Ar or U–Pb age, My ± 2σ	MSWD	SiO_2 wt.%		δ18O, ‰ mineral	Magma calculated	Collected by
Eastern volcanic zone									66	Plag	6.13		
Pauzhetka			27×18	150	300–450								
	83 L-20	Ignimbrite				Plagioclase	0.451 ± 0.022	0.19	70	Qz	7.15	6.57	
		Ignimbrite				Zircon	0.47 ± 0.11 n = 9	0.79	70	Plag	6.04		2
	C-708	Ignimbrite				Plagioclase	0.436 ± 0.056	0.47	73.5	Qz-1	6.82	6.11	
		Ignimbrite				Zircon	0.515 ± 0.071 n = 8	0.57	73.5	Qz-1	6.46		1
									73.5	Plag	5.52		
	K6-3	Ignimbrite				Zircon	0.48 ± 0.19 n = 9	1.7					
	1973E-177	Ignimbrite				Plagioclase	0.441 ± 0.072	0.86		Qz	6.84	6.41	
										Qz	6.94		
									72	Plag	5.96		
	71G-111	Lava, resurgent dome				Plagioclase	0.235 ± 0.041	0.045	72	Plag	4.97	6.36	5
									72	Plag	5.87		
Ksudach	11 M-2002	Ignimbrite	9×9			Groundmass	0.162 ± 0.017	0.06	66	Plag	5.67	5.97	6.7
Gorely			13×9	20	120								
	2006 L-19	Ignimbrite				Obsidian	0.361 ± 0.008	1.15	65	Obs		5.05	2
Karymshina	2007 L-40	Ignimbrite	32×17	1000	800	Plagioclase	1.54 ± 0.09	0.34	73	Qz	7.91	7.13	1.2
						Biotite	1.78 ± 0.02	0.51	73	Plag	6.33		
	2006 L-24	Ignimbrite				Plagioclase	1.68 ± 0.30	0.38	72.8	Qz	7.5	6.66	1
						Biotite	1.78 ± 0.02	0.44	72.8	Qz	7.26		
									72.8	Plag	5.71		
						Zircon	1.763 ± 0.090 n = 8	0.18					
	2005G-5	Ignimbrite				Plagioclase	1.39 ± 0.10	1.12	73	Plag	5.83	5.90	5
									73	Cpx	3.79		
									73	Cpx	4.09		
	2007 L-36	Ignimbrite				Zircon	1.87 ± 0.11 n = 9	0.32	73.4	Plag	6.53	7.06	1.2
	2007 L-32	Post-caldera extrusion				Zircon	0.919 ± 0.084 n = 9	0.26					1.2
Stol Mt	07IB-6	Ignimbrite		40–50	?	Obsidian	3.71 ± 0.08	0.6		Glass	7.18	7.18	1
Karymsky Center: Odnoboky			4×6	15–25									
	2001 L-21	Ignimbrite				Groundmass	0.0694 ± 0.0033	0.38		Glass	5.76	5.76	2
Polovinka			11×11	up to 200	>42								
	1999 L-9	Ignimbrite				Groundmass	0.432 ± 0.0084	0.36		Glass	5.23	5.23	
									76	Qz	6.46	6.01	2
	2007 L-27	Ignimbrite				Plag	55		76	Plag	5.46		1.2

Stena–Soboliny			20×10	10–50	100				68	Plag	5.35	5.77	
	2007 L-22	Ignimbrite				Plagioclase	1.13±0.10	0.46	68	Plag	5.22		
									68	Cpx	4.53		1.2
Korneva River, Karymsky Center													
	509-1	Ignimbrite	?	45	?	Obsidian	1.26±0.01	0.79					4
						Plagioclase	1.24±0.08	0.66	68	Plag	4.58	4.88	
										Plag-1	4.99		
										Plag	5.06		
Bolshoy Semyachik													
	1990 L-8	Ignimbrite without quartz	10×10	Up to 250	42	Plagioclase	0.524±0.082	0.46	64	Plag	6.34	6.51	2
									64	Cpx	5.21		
	1988 L-80	Ignimbrite with Quartz			42	Plagioclase	0.56±0.045	0.15	70.5	Qz	7.47	7.00	2
									70.5	Plag	6.57		
Uzon–Shorokoye Plateau									68	Plag	4.67		
	1990 L-101	Ignimbrite	16×10	5–50	46	Obsidian	0.278±0.017	1.5	68	Cpx	3.1	4.79	2
Zheleznodorozhny Plateau													
	1132-1	Ignimbrite	?	120–160	?	Obsidian	1.29±0.01	0.59	68	Plag	5.85	6.24	4
Sredinny Range													
Khangar			12×16										
	CX1436	Ignimbrite	6			Biotite	0.397±0.008	0.99	74	Plag	6.72	7.57	3
						Plagioclase	0.411±0.07	0.91	74	Plag	7.2		
									74	Plag	7.16		
Nosichan			8										
	PP2240	Ignimbrite				Obsidian	4.02±0.12	0.52	60	Plag	3.24	5.86	3
										Plag	3.89		
Uksichan			12×13										
	ES888	Ignimbrite				Plagioclase	3.56±0.5	0.5	60	Plag	5.1	5.27	3
	ES859	Ignimbrite				Plagioclase	3.34 0.07	0.75	63.9	Plag			3
Tekletunup			5–6		8–9				62	Plag	4.85		
	TT7305	Ignimbrite				Obsidian	5.7±0.16	0.55	62	Cpx	3.74	4.94	3

Late Pleistocene–Holocene Calderas larger than 5 km

Radiocarbon-dated (data from literature)					Years BP				
Kurile Lake	7×12	50	140–170	Radiocarbon	7600	11	71	5.4
Ksudach	5×6		18–19	Radiocarbon	1800		68	4.9
Gorely	13×9	20	120	Radiocarbon	33000	12	65	5.4
Karymsky	5				7900	15	68	5.1
Academy Nauk	4×5			U–Th, fission tracks	18000–48000	14	68	5.2
Maly Semyachik	7			U–Th	15000	14	67	4.6
Uzon	16×10			Radiocarbon	30,000	13	67	4.7
Khangar-II	6			Radiocarbon	39,000	16		
Khangar-III	3×3.5			Radiocarbon	6900	15	67	7.1

Table 2
Whole-rock major and trace element analyses of dated samples and other associated rocks in Kamchatkan Calderas.

Sample		Age ± My	δ18O melt	SiO_2	TiO_2	Al_2O_3	FeO*	MnO	MgO	CaO	Na_2O	K_2O	P_2O_5	Sum	SiO_2 norm
Pauzhetka Caldera															
C-708	Golygin Ignimbrite	0.436 ± 0.056	6.11	72.31	0.272	14.52	2.21	0.074	0.61	2.95	4.20	1.63	0.030	98.81	73.19
1973E-177	"	0.441 ± 0.072	6.41	69.37	0.359	15.36	2.99	0.101	0.96	3.52	4.10	1.68	0.064	98.51	70.42
1983 L-20	"	0.451 ± 0.022	6.57	70.31	0.312	14.78	2.86	0.098	0.48	3.06	4.17	2.00	0.070	98.13	71.64
1971G-111	Ploskaya extrusion	0.235 ± 0.041	6.36	71.70	0.394	13.9	3.3	0.101	0.765	2.72	3.73	2.44	0.03	99.08	72.37
11 M-2002	Ksudach Ignimbrite	0.162 ± 0.017	5.97	65.37	0.780	15.73	5.67	0.200	1.57	4.29	4.83	1.05	0.230	99.72	65.55
2005 L-19	Gorely Ignimbrite	0.3614 ± 0.0083	5.05	65.30	0.932	16.15	4.19	0.162	1.25	3.23	5.33	2.67	0.269	99.48	65.64
Karymshina Caldera															
2007 L-36	Caldera-forming ignimbrite		7.06	70.55	0.283	14.68	1.63	0.039	0.68	2.30	3.80	2.55	0.051	96.56	73.06
-37	"			69.78	0.299	14.62	1.94	0.041	0.65	2.57	3.92	2.56	0.088	96.46	72.33
-38	"			71.64	0.295	14.61	1.32	0.042	0.56	2.49	4.04	2.61	0.065	97.67	73.35
-39	"			71.86	0.296	14.71	1.38	0.064	0.51	2.38	3.99	2.56	0.074	97.83	73.46
-40	"	1.78 ± 0.02	7.13	70.78	0.290	14.69	2.70	0.096	0.60	2.33	4.14	2.56	0.070	98.26	72.03
-41	"			70.00	0.292	14.82	2.75	0.098	0.77	2.30	4.11	2.53	0.081	97.75	71.61
2006 L-24	"	1.78 ± 0.02	6.66	70.29	0.287	14.62	2.25	0.090	0.76	2.79	3.93	2.58	0.083	97.68	71.96
2007 L-43	"			70.20	0.282	14.51	2.05	0.092	0.76	2.69	3.80	2.59	0.082	97.05	72.33
-44	"			70.19	0.287	14.82	2.30	0.100	0.74	2.70	4.17	2.44	0.082	97.83	71.75
-45	"			70.71	0.279	14.76	2.09	0.056	0.67	2.46	4.15	2.70	0.077	97.93	72.20
-46	"			70.10	0.286	14.76	2.24	0.061	0.74	2.64	4.16	2.49	0.082	97.55	71.85
-47	"		7.54	69.95	0.288	15.11	2.31	0.095	0.69	2.79	4.25	2.27	0.080	97.83	71.50
1972 L-321	Zhirovskaya Ignimbrite		7.42	66.01	0.547	15.86	3.89	0.107	1.24	3.14	4.33	2.51	0.133	97.77	67.52
2007 L-35	Post-caldera extrusion			73.22	0.184	12.99	1.23	0.079	0.34	1.33	3.96	3.39	0.047	96.77	75.66
2007 L-32	"			77.40	0.180	12.10	1.62	0.064	0.34	1.28	3.24	3.20	0.043	99.46	77.82
2005G-5	Bannaya R Ignimbrite	1.39 ± 0.10	5.88	62.91	0.625	16.22	4.57	0.116	1.65	4.65	3.77	2.09	0.179	96.77	65.01
Calderas of the Eastern Volcanic zone															
07-IB-15	Stol Mt pumice			56.66	1.169	16.38	8.97	0.212	3.01	6.68	4.08	1.26	0.273	98.70	57.41
07-IB-6	Stol Ignimbrite	3.71 ± 0.08	7.18	57.70	1.156	16.18	8.55	0.208	2.89	6.34	4.36	1.28	0.305	98.97	58.30
2001 L-21	Odnoboky Ignimbrite	0.0694 ± 0.0033	5.76	70.73	0.347	14.19	2.46	0.088	0.69	2.26	4.50	2.72	0.084	98.07	72.12
1999 L-9	Polovinka Ignimbrite	432 ± 84	5.23	63.91	0.809	15.46	5.90	0.175	1.77	4.46	4.72	1.66	0.178	99.03	64.53
2007 L-27	Polovinka Ign			76.90	0.16	11.40	1.41	0.08	0.30	1.24	2.85	3.26	0.03	97.63	78.77
2007 L-22	Stena–Soboliny	1.13 ± 0.10	5.77	66.60	0.857	15.16	4.64	0.147	1.13	3.44	4.53	2.30	0.191	98.99	67.28
2006 L-6	Stena–Soboliny			67.20	0.733	15.20	3.83	0.149	1.18	3.24	4.75	2.28	0.160	98.71	68.08
509-1	Korneva R ignimbite	1.26 ± 0.01	4.88	68.19	0.767	14.79	3.89	0.141	0.87	2.87	4.71	2.51	0.164	98.91	68.94
1988 L-80	B Semiachik ign	0.56 ± 0.045	7.00	74.44	0.210	13.06	1.49	0.064	0.40	1.74	3.98	2.74	0.035	98.15	75.84
1990 L-8	B Semiachik ign	0.524 ± 0.082	6.51	63.82	0.990	15.56	6.76	0.150	1.88	4.38	3.86	1.98	0.230	99.38	64.22
1990 L-101	Uzon Ignimbrite	0.278 ± 0.017	4.79	67.21	0.731	15.09	4.30	0.157	1.10	3.32	4.98	1.77	0.181	98.83	68.01
1132-1	Plateau ZhD	1.29 ± 0.01	6.24	67.03	0.467	15.74	3.45	0.090	1.23	4.00	4.25	1.63	0.098	97.99	68.41
Caldera-forming ignimbrites of Sredinny Range															
CX1436	Khangar	0.398 ± 0.008	7.57	72.16	0.244	13.62	1.50	0.075	0.36	1.16	4.04	3.69	0.080	96.92	74.45
PP2240	Noksichan	4.02 ± 0.12	5.86	58.36	1.002	16.50	6.65	0.136	2.49	5.27	3.80	1.97	0.313	96.49	60.49
ES888	Uksichan	3.56 ± 0.50	5.27	58.11	1.055	16.43	6.87	0.168	2.31	4.84	3.97	3.58	0.609	97.93	59.33
ES859	Uksichan	3.34 ± 0.07		63.90	0.930	16.59	3.94	0.160	0.96	2.46	4.57	5.07	0.280	98.86	64.64
TT7305	Teklentunup	5.70 ± 0.16	4.94	57.64	0.854	16.91	5.39	0.192	2.07	4.33	4.10	4.32	0.478	96.28	59.87

characteristics for future compilations. Additionally, we compare this new geochronological data on large calderas with marine ash records along the coasts of Kamchatka in order to identify the largest explosive eruptions in the marine record.

2. Methods

Samples of large-volume ignimbrites that are found in the vicinity of major caldera complexes in Kamchatka were collected by authors of the paper in the course of a decade-long investigation. We collected and geochemically characterized more samples than we dated (Tables 1 and 2) as each sample went through rigorous investigation based on the freshness in both hand specimen and thin section. In particular, we selected rocks with large, fresh feldspars and biotites without visible crystal clots for incremental heating analyses and densely welded groundmass and obsidianic samples for step-heating experiments. For zircon extraction, samples totaling 1 kg were crushed and treated with HF to dissolve glass attached to zircons, followed by density separation in heavy liquids and mineral picking.

The $^{40}Ar/^{39}Ar$ analyses were performed at the University of Wisconsin–Madison Rare Gas Geochronology Laboratory. Individual biotite phenocrysts and/or multi-crystal aliquots of plagioclase were fused using a 25 W CO_2 laser (5–16 fusions per sample). Obsidian separates (100–137 mg) were incrementally heated in a double-vacuum resistance furnace following the procedures of Jicha and Singer (2006). Because isochron regressions agreed with plateau ages and did not reveal evidence that excess argon or low temperature-alteration was significant in any of the samples, we consider the weighted mean plateau ages to give the best estimate of the time elapsed since eruption.

U–Pb dating of zircons was performed using Cameca 1270 ion microprobe at UCLA. Typically, 20–30 zircon grains from each sample were hand-picked, mounted in epoxy, polished to ~75% of their midsection, and mapped in reflected light and back-scatter electron microscopy. We followed standard analysis protocols for the analysis of youthful zircons (Schmitt et al., 2003a; Bindeman et al., 2006). Ion intensities were measured in 12–15 cycles using a mass-filtered O– primary ion beam of ~15 nA focused to an oval 25–30 μm spot. AS-3 (Paces and Miller, 1993) reference zircons were used to calibrate U, Th, and Pb sensitivities. Measured ages were adjusted for the initial U–Th disequilibria using techniques described in Schärer, 1984; Reid, 2003, and Bindeman et al., 2006 which increase the age by ~80 ky.

Cr	Sc	V	Ba	Rb	Sr	Zr	Y	Nb	Ga	Cu	Zn	Pb	La	Ce	Th	Nd	U
3	6	35	497	27	241	103	10	0.8	12	5	33	7	6	14	1	9	2
4	8	57	521	25	276	102	12	1.8	12	10	45	8	8	14	1	7	0
4	6	53	572	32	231	110	13	1.8	15	7	34	7	9	20	3	9	0
0	82	352	14	311	139	119	45	2.2	23	39	85		9	22	1	19	1
2	17	45	783	47	348	270	48	7.9	18	4	81	10	23	55	3	33	1
3	5	28	783	51	261	94	12	1.7	14	5	27	8	12	24	4	9	2
3	6	40	807	51	274	100	13	2.3	14	5	37	8	13	24	4	11	2
4	6	32	793	51	274	97	12	3.3	13	4	23	9	10	22	4	9	2
4	4	29	801	51	274	98	13	2.9	13	3	25	8	15	28	3	12	0
3	5	40	783	52	277	95	13	1.8	13	5	30	8	13	23	3	11	1
4	5	45	790	50	272	98	12	2.4	14	5	41	7	9	22	3	10	1
4	5	36	791	53	280	98	15	2.5	12	5	35	7	12	26	4	13	2
3	5	37	782	55	268	97	12	2.7	14	5	33	9	11	29	3	12	2
4	5	36	779	49	288	97	13	2.2	13	5	41	14	15	23	3	10	3
3	5	36	822	55	263	98	14	2.4	14	4	35	8	15	26	3	14	2
3	6	38	786	49	285	98	12	2.4	13	5	33	6	12	22	4	12	1
3	7	41	748	45	300	100	13	1.9	14	4	37	7	12	24	2	12	2
5	11	78	729	49	310	182	22	3.9	16	17	55	11	14	31	3	18	1
2	4	14	909	67	143	86	14	3.9	13	1	25	11	17	31	5	13	3
6	14	108	651	40	449	151	21	2.9	17	24	62	8	12	23	3	14	2
1	30	258	238	17	402	105	30	2.9	17	172	98	1	9	24	0	19	2
2	29	227	255	19	392	113	30	3.2	16	129	100	2	10	26	0	18	2
1	8	37	581	41	196	141	26	2.7	13	7	41	7	14	27	2	16	3
2	22	116	411	24	328	152	35	1.8	17	28	98	6	15	26	1	19	3
7	17	71	581	37	269	199	39	4.6	16	20	88	8	15	37	1	25	2
5	16	59	545	40	273	183	36	3.3	17	8	81	8	12	32	2	21	1
2	16	44	618	41	245	215	39	4.8	17	15	78	7	18	34	2	24	2
4	3	22	741	52	177	87	10	1.6	11	3	23	5	11	16	2	8	1
3	18	45	443	30	219	167	38	3.8	17	8	83	7	10	23	0	17	1
11	66		391	35	201	183	34	2.3	16	13	57	6	16	31	2	19	0
5	3	18	744	72	146	156	16	13.9	15	5	42	10	18	43	9	17	3
14	19	167	770	28	566	107	22	4.3	16	36	70	8	17	32	1	18	2
1	22	176	1231	55	561	190	33	4.5	18	29	104	12	18	46	1	33	2
			1300	46	420												
4	16	141	2161	60	801	142	29	2.3	16	29	108	21	27	51	4	31	2

Oxygen isotope analyses were performed at the University of Oregon stable isotope lab using CO_2–laser fluorination (e.g. Bindeman, 2008). Individual and bulk mineral grains ranging in weight between 0.6 and 2 mg were reacted in the presence of purified BrF_5 reagent to liberate oxygen. The gas generated in the laser chamber was purified through a series of cryogenic traps held at liquid nitrogen temperature, and a mercury diffusion pump was used to remove traces of fluorine gas. Oxygen was converted to CO_2 gas in a small platinum–graphite converter, the yield was measured, and then CO_2 gas was analyzed on a MAT 253 mass spectrometer. Four to seven standards were analyzed together with the unknowns during each analytical session. San Carlos olivine ($\delta^{18}O = 5.35‰$) and Gore Mt. Garnet ($\delta^{18}O = 5.75‰$) were used. Day-to-day $\delta^{18}O$ of standards ranged from −0.1 to −0.25‰ than their empirical value and therefore unknown samples were adjusted to correct for this small day-to-day variability on the SMOW scale. The precision on standards and duplicates of individual analyses is better than 0.1‰.

Major and trace element whole-rock X-ray fluorescence (XRF) analyses were done at the GeoAnalytical Lab at Washington State University on their ThermoARL Advant'XP + sequential X-ray fluorescence spectrometer. Sr and Nd isotope analyses were obtained by TIMS at the Institute of Earth Sciences, Taipei, Taiwan. The matrix of each crushed sample was picked up under a stereo microscope and analyzed for the isotopic compositions of Sr and Nd using established techniques (Chen et al., 1990, 1993).

3. Results

The results of Ar–Ar dating of ignimbrite sheets along with the estimated sizes of their calderas and their estimated volumes are given in Table 1; compositional and oxygen isotopic parameters are given in Table 2. Below, we describe each caldera complex with emphasis on the three largest Pleistocene eruptions: the Golygin Ignimbrite, Karymshina Ignimbrite and the multi-caldera Ksudach Volcano.

4. Major calderas of the Eastern Volcanic Front

4.1. Golygin Ignimbrite and Pauzhetka Caldera

The Pauzhetka Depression measures 27 × 18 km (Fig. 3) and has vertical displacements of close to 1000 m (Melekestsev, 1980; Erlich, 1986). The caldera-forming Golygin Ignimbrite is preserved around the Pauzhetka Depression (Fig. 3) as a sugar-white to pale, densely welded to pumiceous deposit with a total thickness of 20–30 m, approaching 100 m in the northern portion of the inferred caldera. The geothermal drill core drilled in the center of Pauzhetka Caldera has identified a 125–

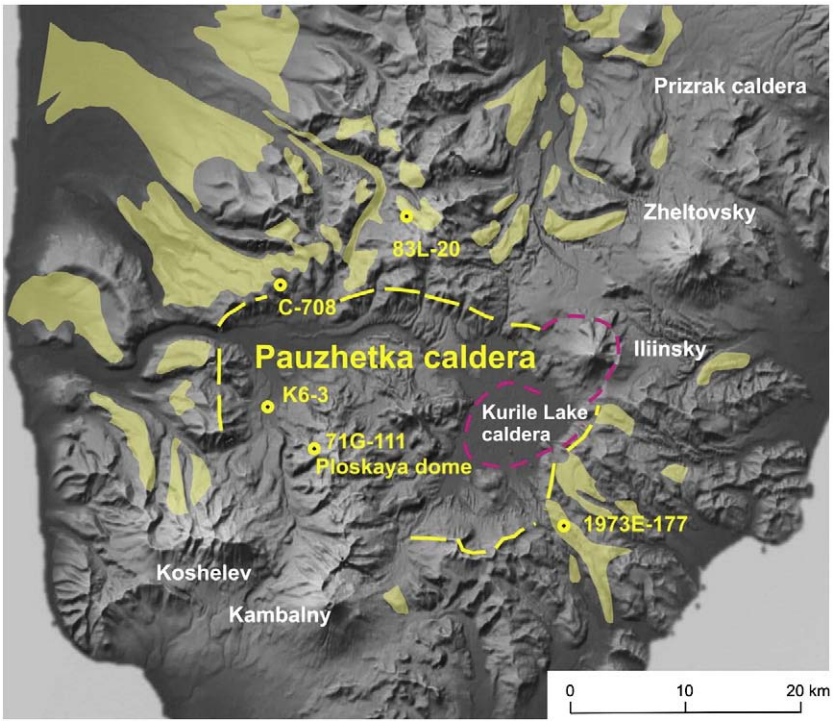

Fig. 3. Eroded Golygin ignimbrite sheet associated with Pauzhetka Caldera (transparent yellow). Location of this area is shown by Frame 3 in Fig. 1. Outlines of the ignimbrite lobes are according to Melekestsev et al. (1974) and Leonov (1989). Location of this area is shown by Frame 3 in Fig. 1. Yellow dashed line shows the 0.45 Ma Pauzhetka Caldera rim where expressed in topography. Location of dated samples is shown with yellow circles. Magenta dashed line shows the rims of the Holocene Kurile Lake Caldera and presumed landslide crater, pre-dating Iliinsky Volcano; for dispersal of the Holocene ignimbrite (see Fig. 6 in Ponomareva et al., 2004).

190 m thick inracaldera tuff layer overlain by 800 m thick volcano–terrigenic material (Erlich, 1986; Leonov, 1989). Previous geochronologic dating efforts of the Golygin Ignimbrite by Masurenkov (1980) and Kozhemyaka and Ogorodov (1977) yielded diverse ages ranging from 1.5 My to 0.2 Ma with the later age preferred by the authors. The uncertain dating resulted in the hypothesis that Pauzhetka represents a volcano–tectonic depression, formed over a long time, by a series of eruptions, rather than a collapse caldera. Gravity investigation (Masurenkov, 1980; Erlich, 1986) identified a gravity deficiency coinciding with the caldera boundaries while seismic methods and drilling in the caldera identified the Cretaceous basements at 2 km depth. The composition of the Golygin Ignimbrite (Table 2) is rhyolitic and it contains large quartz phenocrysts. Rhyolites with abundant quartz phenocrysts are rare in Kamchatka and other island arcs.

The Ar–Ar ages of three samples taken from three separate extracaldera ignimbrite lobes (Table 1) yielded overlapping ages within uncertainties, with an average age of 443 ± 8 k.y. (1 st dev). The U–Pb zircon dating of two samples from ignimbrite lobes and one sample from a 190 m thick intracaldera tuff from the drill core also yielded overlapping ages with an average U–Pb zircon crystallization age of 488 ± 24 k.y. (MSWD = 0.47). Concordance between U–Pb zircon ages of extracaldera and intracaldera facies firmly establishes the age of Pauzhetka Caldera, with the 443 ± 8 k.a. Ar–Ar age as the preferred eruption age of the large-volume Golygin Ignimbrite because zircon U–Pb ages typically predate Ar–Ar eruption ages by a few tens of thousand years (e.g. Reid et al., 1997; Bindeman et al., 2006; Simon et al., 2008).

These new geochronologic data, compositional and isotopic similarity of rhyolitic samples, and the radial distribution of extracaldera ignimbrites around the 20–25 km Pauzhetka Depression with their inferred directions of flow (Fig. 3) suggests that the Golygin Ignimbrite erupted in a single episode causing the formation of the Pauzhetka Caldera. Following the caldera collapse, a combination of post-caldera resurgence and regional tectonism has resulted in the formation of Kambalny Horst (ridge north of Kambalny volcano, Fig. 3), 250–400 m above the caldera moat, which cross-cuts the southern caldera boundary and uplifted precaldera basaltic rocks.

Given the caldera area and an estimated 1 km vertical downdrop, the volume of erupted products is estimated to be at least 450 km^3. Alternatively, adding 1) the exposed volume of extracaldera Golygin Ignimbrite (100 km^3; Sheimovich, 1979); and the Pauzhetka Intra-Caldera Ignimbrite (200–300 km^3; Sheimovich, 1979) yields estimates approaching 400 km^3. Other estimates of exposed extracaldera ignimbrite volumes are 70–80 km^3 (Kozhemyaka and Litasov, 1980), which combined with our intracaldera ignimbrite volume of 60–80 km^3 yields an estimated 130–160 km^3 of known volcanic products. Given the density of the Golygin Ignimbrite (about 2 g/cm^3) this would correspond to 100–125 km^3 DRE (dry rock equivalent) of magma. Taking into account ash loss using the relationship that ash constitutes 50% of the total erupted volume of rhyolitic arc magmas as demonstrated at Mt Mazama (Bacon, 1983), then the total volume of eruptive products at 443 ka is close to 300 km^3, or perhaps closer to 200 km^3 of magma. The latter estimate is also more realistic for the volume of Pauzhetka Caldera. Thus, the caldera-forming eruption of the Golygin Ignimbrite in Pauzhetka Caldera represents the largest known eruptive episode in Kamchatka during the past 1 Ma.

The 50 km^3 of new, post-caldera silicic lavas (Kozhemyaka and Ogorodov, 1977) are represented by two extrusions (Leonov, 1989), with the most prominent unit, the Ploskaya (Flat) Extrusion, which has a rhyodacitic composition without quartz, constituting part of the resurgent dome. Its newly-determined Ar–Ar age is 235 ± 4 ka (Table 1). It appears that the silicic magma was largely exhausted following the collapse from the Golygin Ignimbrite eruption and small-volume post-caldera silicic volcanism. Late Pleistocene eruptions of basaltic lava resulted in the formation of small stratocones while the large basaltic volcanoes of Koshelevsky and Kambalny were formed on the inferred rim boundaries outside of the caldera (Fig. 3).

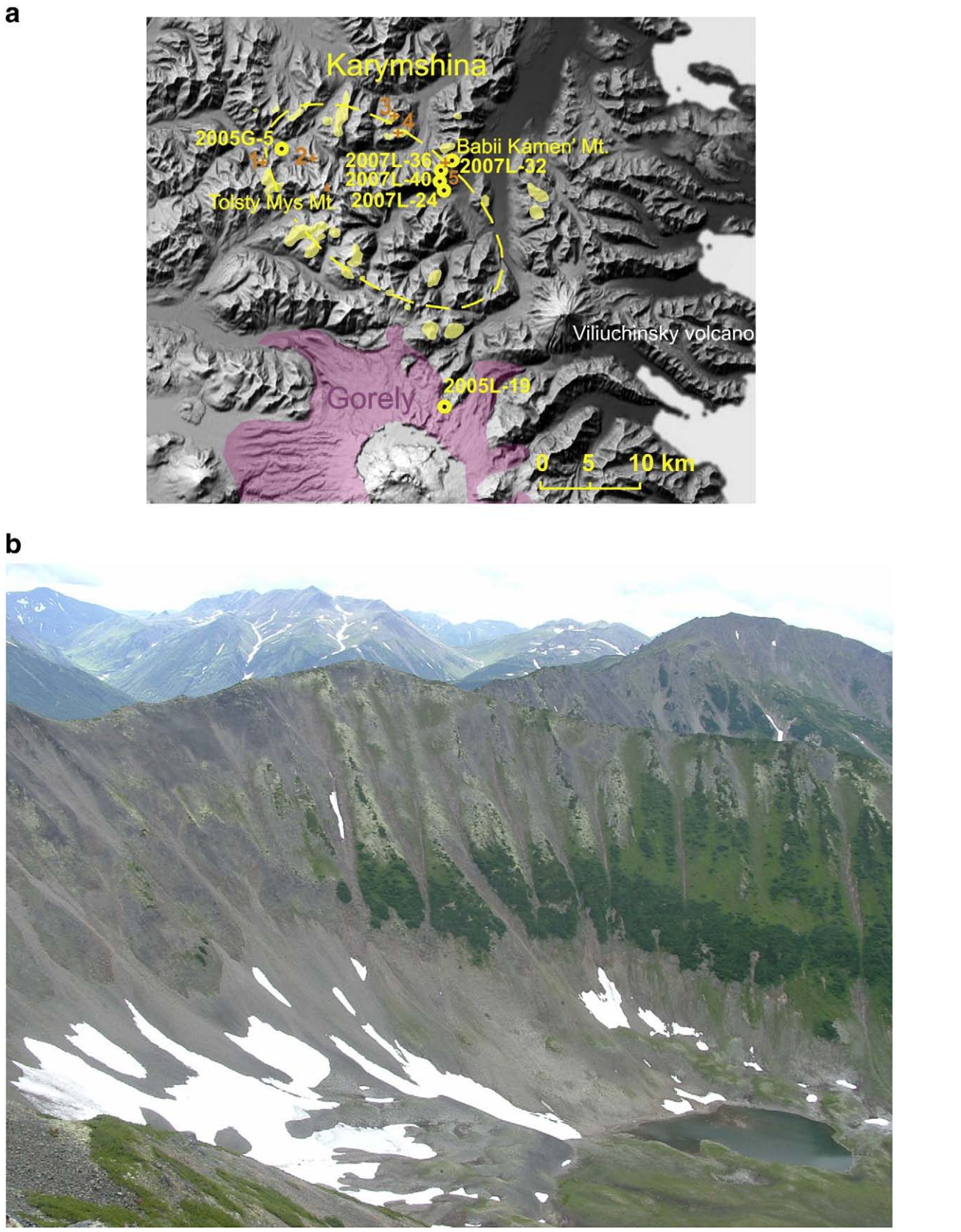

Fig. 4. a) Eroded ignimbrites sheet, caldera fill, extrusive domes, and inferred boundaries of the 1.78 Ma Karymshina Caldera and northern part of the ignimbrite sheet related to Gorely Caldera (pink) with sample locations dated by Ar–Ar and U–Pb methods. Samples 2006 L-24, 2007 L-40, 2007 L-36 represent a single cross section of geochemically homogeneous intracaldera ignimbrite, see Table 1 for geochronologic and geochemical cross-sections through this ignimbrite; Tolsti Mis (Fat Peninsula) is interpreted to represent the resurgent dome of Karymshina Caldera. Inferred caldera boundaries of the 1.78 Ma Karymshina Caldera are after Leonov and Rogozin (2007). Ar–Ar ages of ring-fracture caldera extrusions as determined by Sheimovich and Golovin (2003); 1 — 0.53 ± 0.05 Ma; 2 — 0.63 ± 0.03 Ma; 3 — 0.81 ± 0.02; 4 — 0.69 ± 0.02; 5 — 0.5 ± 0.2. b) View to the west from the Babi Kamen' extrusion into the glacially eroded 1000 m thick intracaldera ignimbrites and extrusions of Karymshina Caldera.

The 443 ka caldera-forming eruption was the first in the series, as Pauzhetka represents a nested caldera complex that includes the subsequent eruption of the Kurile Lake Ignimbrite and formation of the 7×12 km Kurile-Lake Caldera (Fig. 3b, 7.6 ky, >140–170 km^3 tuffs, >60 km^3 DRE, Ponomareva et al., 2004). Additionally, silicic volcanism continued in the Holocene and resulted in the formation of intracaldera extrusions of rhyodacitic to dacitic composition, such as Dikiy Greben' Volcano, with a total volume of silicic rocks from 10–15 km^3 (Bindeman and Bailey, 1994), and dacitic flows in Iliinsky Volcano.

Oxygen isotope investigation of phenocrysts in the Golygin Ignimbrite, Ploskaya Lavas, Kurile Lake deposits, and Late Holocene eruptive products including those from Iliinsky and Dikiy Greben' Volcanoes, reveals a zig-zag pattern superimposed on an overall decrease in δ^{18}O with younger age (see Bindeman et al., 2004, Fig. 7a). As volcanic rocks in Iliinsky Volcano are low-δ^{18}O, their source is likely to be inside Pauzhetka Caldera and the inferred boundary of a hypothetical Late Pleistocene caldera (Fig. 3). The Golygin Ignimbrite represents low-K, normal to subtly high-δ^{18}O magma with a nonradiogenic Sr isotopic value of 0.703255 ± 0.000015 (Bindeman et al., 2004), indicative of derivation by fractional crystallization of more mafic parents or remelting of young crust. As in Ksudach Volcano described later in this paper, eruptions from a nested caldera complex resulted in burial of low-δ^{18}O, hydrothermally-altered intracaldera fill by caldera collapse and loading. Subsequent magmas are able to interact with these low δ^{18}O materials, thus becoming progressively lower in δ^{18}O.

4.2. Karymshina (Bolshe-Banny) Caldera

The Karymshina "ring structure" was discovered during exploration of Bolshe-Banny geothermal field in late 1960s (Erlich, 1986 and earlier references within), and later redefined as a large volcano–tectonic structure (Lonshakov, 1979). The Karymshina River large silicic center in east-central Kamchatka is represented by a ~1000 m thick layer of rhyolitic ignimbrite and about a dozen surrounding extrusive domes of high to low- silica composition (Fig. 4). The presence of quartz and biotite in rhyolites from the Karymshina Center distinguishes these old uplifted Early Pleistocene rocks from the biotite and amphibole-free Holocene lavas of the surrounding volcanoes in the EVF. Previous researchers (Sheimovish and Khatskin, 1996; Sheimovish and Golovin, 2003) reported K–Ar dates of these extrusive domes ranging from 0.5 to 2.2 Ma. They also dated samples of ignimbrites spanning from 4.2 to 1.2 Ma, with the majority of dates

Table 3
New isotope analyses of rocks from Ksudach Volcano and Karymshina Caldera.

blue- previously published (Bindeman et al, GCA 2004)

	Unit	Age, k.y.	Volume km3	SiO2	δ^{18}O, mineral	δ^{18}O magma	^{87}Sr/ ^{86}Sr	10>-6	^{143}Nd/ ^{144}Nd	10>-6	eNd
Ksudach Volcano											
Extracaldera, closest basaltic cone outside of Ksudach, Zheltaya Mt											
6M-2002/1				61.50	5.78 (Plag)	5.80	0.703496	59	0.512982	6	6.67
proto-Ksudach shield volcano (Ksudach 1-1)											
02IPE-49		324±160			5.67 (Plag)	5.90					
Earliest caldera-forming eruption											
11M-2002/2	KS5	162±17	>>10?	65.50	5.67, 6.13 (Plag) 4.13 (Cpx)	5.50	0.703298	55	0.513063	7	8.25
Post-Caldera, intracaldera lavas, basaltic cinder cones											
02IPE-13					5.5 (Plag) 4.92 (Cpx)	5.60	0.703333	51	0.513057	8	8.13
02IPE-14					5.29 (Plag) 4.63 (Cpx)	5.30	0.703322	57	0.513059	8	8.17
Pleistocene Caldera-forming Eruption		<162, >8.8	?								
02IPE-15					5.02 (Plag) 3.72 (Cpx)	4.98	0.703318	46	0.513056	8	8.11
02IPE-16					5.21 (Plag) 4.21 (4.21)	5.55	0.703300	54	0.513065	6	8.29
Early Holocene caldera-forming eruption											
C977a	KS4	8800 BP	1.5-2	63.22	5.01 (Plag) 4.09 (Cpx)	5.11	0.703321	52	0.513076	6	8.50
C977	KS4			62.99	4.94 (Plag)		0.703318				
mid-Holocene caldera-forming eruptions											
8889/2 KS3	KS3	6300 BP	0.5-1	69.55	4.92 (Plag) 3.96 (Cpx)	5.19	0.723348	51	0.513063	6	8.25
8889/3 KS3		6300 BP		62.79	5.12 (Plag)	5.11					
86039/14 KS2	KS2	6000 BP	7-8	62.57	5.02 (Plag) 3.71 (Cpx)	5.01	0.703310	50	0.513072	10	8.43
C918	KS2	6000 BP		62.44	5.64 (Plag) 4.64 (Ol)	5.62	0.703312				
post KS2 intracaldera lava Paryashii Utes											
C953				65.35	4.75 (Plag) 3.74 (Cpx)	4.87	0.703370				
late Holocene caldera-forming eruption KS1											
8880/5	KS1	1800 BP	18-19	71.80	4.68; 4.69 (Plag) 3.46 (Cpx)	4.89	0.703389				
post KS-1 intracaldera lavas											
C999	lava	>1600 BP		54.18	5.15 (plag) 4.21 (Cpx)	4.97	0.703311				
KA110-7	lava	<1500 BP		58.68	5.41 (WR)	5.41	0.703220				
KA1/7	dome	<1500 BP		56.79	5.74 (WR)	5.74	0.703260				
Shtyubel Cone eruption 1907 AD											
8882/2	Ksht	1907 AD	0.8-1	68.45	5.56 (Plag) 4.66; 4.56 (Cpx)	5.80	0.703276				
Nodules and xenoliths											
KS-alliw	Ol-An cumulate			50.00	5.20 (Plag) 4.63 (Ol)	5.33	0.703310				
KA-38a/7	xenolith			49.35	5.84 (WR)	5.84	0.703310		0.513070		8.39
KA25A-7	xenolith			67.15	5.09 (WR)	5.09	0.703250		0.513063		8.25
KA39/7	xenolith			48.21	5.62(Plag) 4.43 (Cpx)	5.06	0.703390				
Karymshina Caldera											
Bannaya R Ignimbrite											
2005G-5				62.90	5,76 (Plag) 3,79; 4,09 (Cpx)	5.90	0.703324	10	0.513065	12	8.29
Karymshina R Ign, mid-lower portion											
2007L-40				70.78	7,91(Qz), 6,33 (Plag)	7.13	0.703317	8			
Karymshina R Ign, upper portion											
2007L-36				70.55	6,53 (Plag)	7.06	0.703328	10	0.513048	12	7.96
Zhirovskaya Ignimbrite											
1972-L321				66.01	7,72(Qz), 7,12 (Plag)	7.42	0.703320	8	0.513015	12	7.32

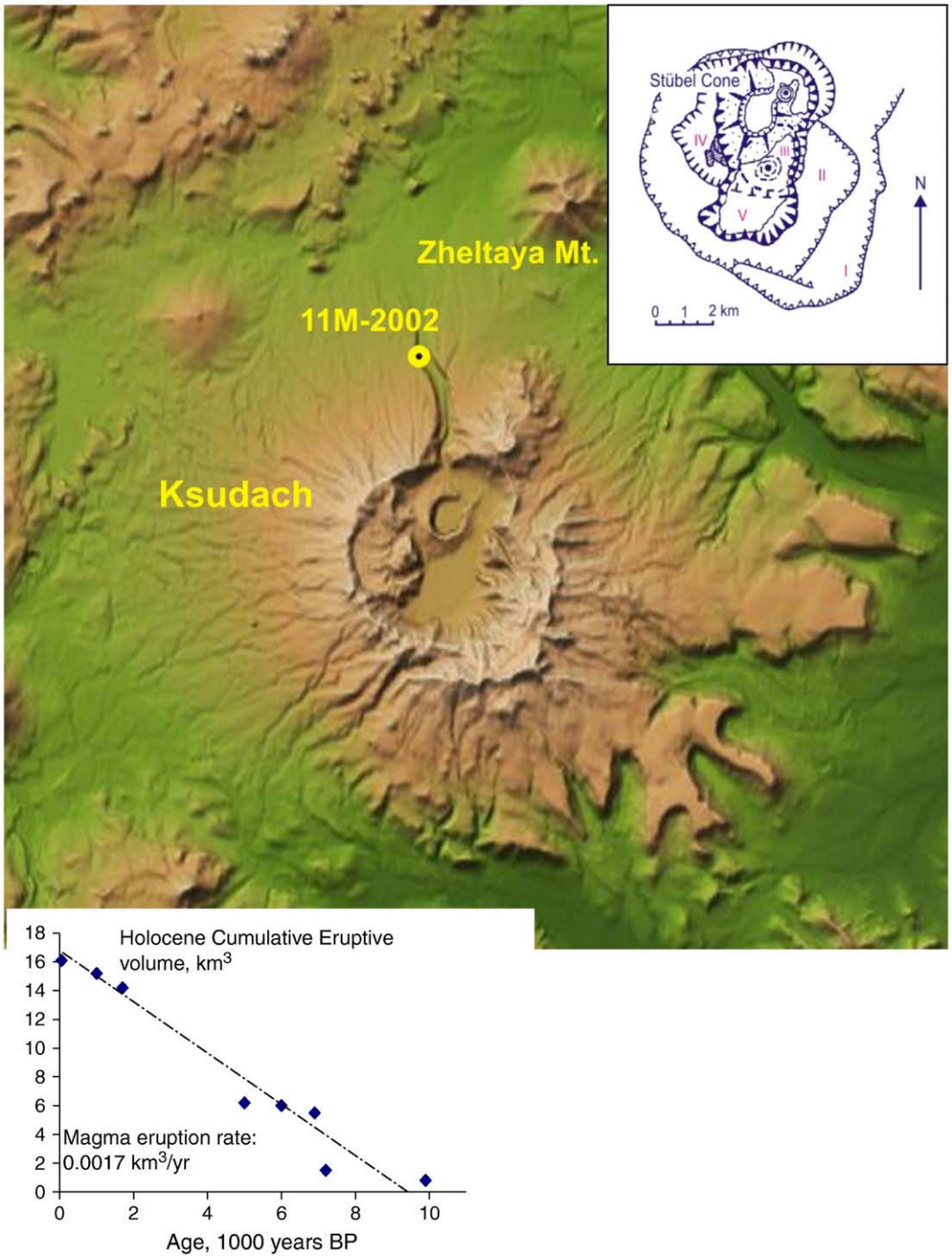

Fig. 5. Ksudach Multi-Caldera Volcano showing overlapping caldera boundaries, ignimbrite sheets and location of a newly dated sample of the oldest ignimbrite. Location of this area is shown by Frame 6 in Fig. 1. Holocene (III–V) and Pleistocene (I–II) caldera boundaries are after Volynets et al. (1999). Lava domes (concentric cupola) and the young Stübel Cone volcano are shown in the inset. Lower inset shows estimated Holocene magma eruption volumes (DRE equivalent).

ranging from 1.2 to 1.52 Ma, and concluded that the area is represented by a series of extrusive domes erupted approximately 2 Ma or more. Leonov and Rogozin (2007) reinterpreted silicic rocks from the Karymshina River as consisting of voluminous caldera-forming ignimbrites and post-caldera ring-fracture domes, thus identifying a large-scale Early Pleistocene caldera (Fig. 4). The presently uplifted and eroded caldera floor (Fig. 4b) exposes only intracaldera ignimbrites, but the search for extracaldera ignimbrites is continuing. The latter are expected to be eroded but might be present under the volcanic edifices of neighboring stratovolcanoes. The 100–120 m thick extracaldera Karymshina Ignimbrite was found under Zhirovskoy Volcano, whose lavas are dated at 0.67 to 0.84 Ma by K–Ar method (Sheimovich and Karpenko, 1996).

In the field, ignimbrites are distinguished from the domes by the existence of subhorizontal fiamme. The domes form topographic highs around the inferred intracaldera Karymshina Ignimbrites, defining an ellipsoidal pattern (Fig. 4). Furthermore, Tolsty Mys mountain is exposed in the center of the inferred caldera boundaries and is represented by uplifted intracaldera ignimbrite interpreted to represent a resurgent dome (Leonov and Rogozin, 2007).

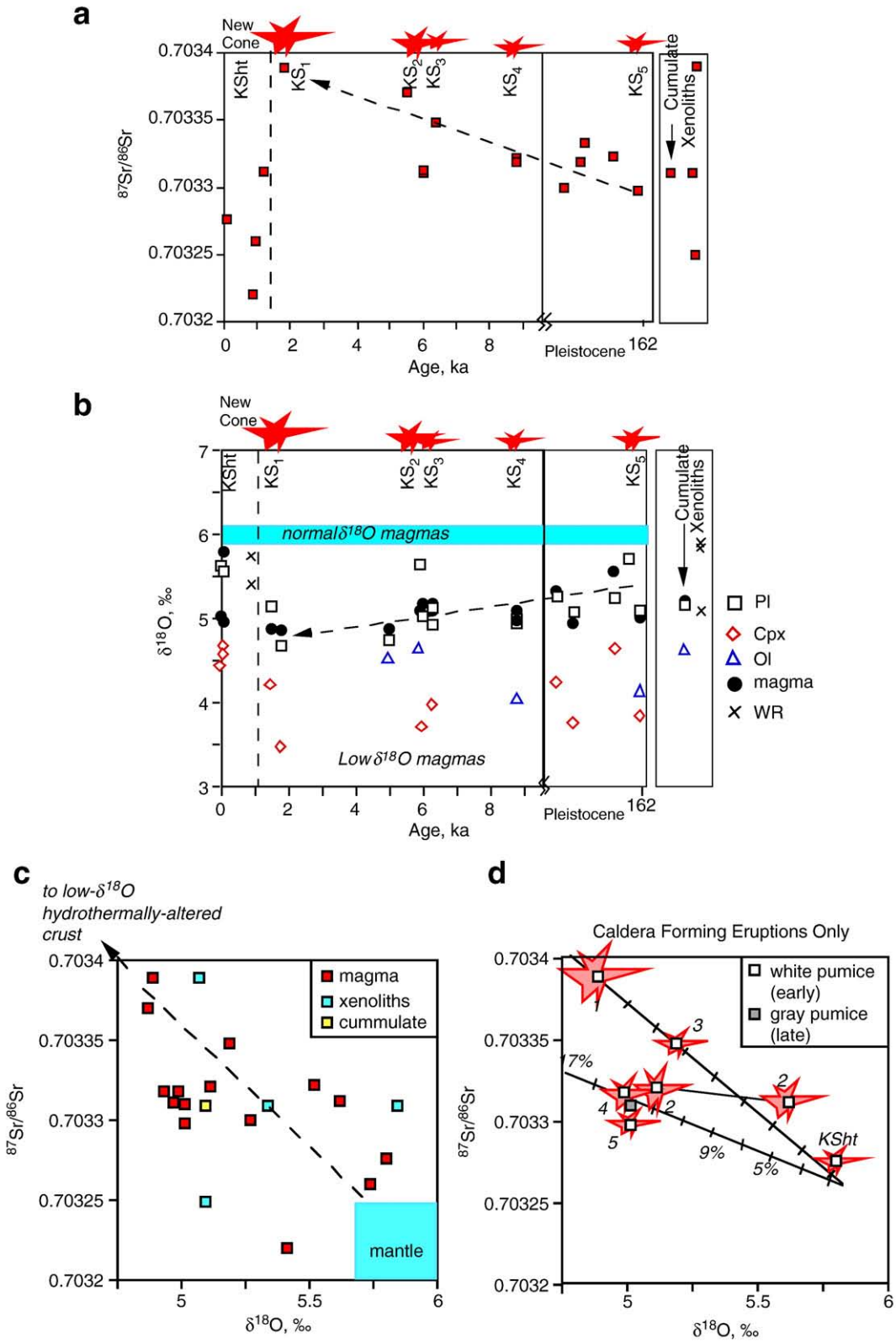

Fig. 6. Isotopic evolution of Ksudach magmas. a,b) Evolution of O and Sr isotopes in tephras and lavas erupted in the nested caldera complex of Ksudach volcano. Holocene ages were determined by ^{14}C. Notice that magmas become lower in $\delta^{18}O$, which indicates progressively greater assimilation of low-$\delta^{18}O$ hydrothermally-altered rocks. At the same time increases in Sr isotopic ratio indicate that assimilated rocks are older, more radiogenic and/or were altered by waters that circulated through the most radiogenic Cretaceous basement. Stars represent five episodes of caldera-forming eruptions. Notice that caldera formations KS5–KS2 did not disturb the magma chamber completely. KS1 eruption (18 km^3) was the largest and the youngest. It apparently emptied the entire magma chamber. After KS1 the intracaldera Stübel Cone started to form with the most recent 1 km^3 eruption in 1907. Post KS1 magmas have more normal $\delta^{18}O$ and are less radiogenic with respect to Sr. c,d) Sr–O isotopic relationship suggests a 0.7036 and 0‰ assimilant end-member. This Sr isotopic composition does not match Cretaceous basement rocks (0.706), but matches heavily altered younger rocks (~0.7036–0.704), possibly proto-Ksudach volcanic pile altered by hydrothermal activity. The proportion of 0‰ assimilant in mantle-derived magmas changes from 15% in KS1, to 3% in the Ksht 1907 AD eruption products.

It is important to determine whether the eroded Pleistocene ignimbrites represent products of a single large-volume eruption or a series of smaller eruptions, as suggested earlier by Sheimovich and Khatskin (1996). In order to resolve this, we sampled the top and the bottom of the exposed rhyolitic intracaldera ignimbrite section in the eastern flank of the caldera and determined their Ar–Ar ages (Table 1). Biotite crystals from both samples yielded identical ages of 1.78 ± 0.02 Ma (MSWD = 0.51) while plagioclase showed 1.54–1.68 Ma ages that overlap with the more precise biotite age within 2 sigma uncertainty. Zircon crystals from the top sample yielded a U–Pb age of 1.87 ± 0.11 Ma (MSDW = 0.32, $n = 9$), with no evidence of inheritance. This zircon crystallization age overlaps with the 1.78 Ma Ar–Ar biotite age which we adopt as the eruption age. It appears that the 1000 m thick sequence of intracaldera ignimbrites was formed in the course of a single eruption or, pending better dating and geological study, a rapidly emplaced sequence of compositionally and mineralogically similar ignimbrites, beyond analytical resolution of Ar–Ar geochronology. Plagioclase from an intracaldera ignimbrite (sample 2005G-5) on the northwest side of the caldera near Bannaya River (Fig. 4) yielded an Ar–Ar age of 1.39 ± 0.10 Ma. Additional age constraints are needed to determine if this dacitic ignimbrite is identical in age to the extracaldera dacitic ignimbrite (sample 426-L-1972) that yielded a 1.62 ± 0.21 Ma Ar–Ar age from a Novosibirsk geochronology laboratory and could represent a younger caldera-forming episode at Karymshina Caldera. U–Pb zircon ages of one topographically-prominent extrusion Babii Kamen' average 0.92 ± 0.08 Ma age (MSDW = 0.26, $n = 9$), significantly younger than the age of the intracaldera ignimbrites it intruded. Other high-silica–rhyolitic extrusions previously dated by K–Ar and Ar–Ar to be younger than 1 Ma are shown on Fig. 4.

The high-silica rhyolitic compositions of these extrusions, which is rare in Kamchatka, and their broad geochemical similarity with the Karymshina Ignimbrite suggests that they may represent post-caldera ring-fracture extrusions from the remobilized Karymshina reservoir. Oxygen isotopic investigation of the Karymshina Ignimbrite and postcaldera intrusions yielded nearly identical normal to high-$\delta^{18}O$ values (Table 2) while newly-determined Sr and Nd isotopic ratios for the ignimbrite are 0.703317–0.703328, and 0.513015–0.513065 respectively (Table 3).

4.3. Calderas of the Ksudach eruptive center and magma evolution

The multi-caldera Ksudach Volcano (Fig. 5) has been studied in great detail with respect to whole-rock isotopic variations of O, Sr and Nd (Table 3) and whole-rock and mineral chemistry (Volynets et al., 1999; Bindeman et al., 2004; Andrews, 2009). Ksudach Volcano is one of the most explosive Holocene volcanoes in Kamchatka and had three episodes of caldera formation during the Holocene; 8800 BP (Caldera III; tephra code KS_4; >2 km^3 of tephra), 6300 BP (KS_3, 1 km^3) and 6000 BP (Caldera IV; tephra code KS_2, 7–8 km^3), and 1800 BP (Caldera V; KS_1, 18–19 km^3). These tephras are widely used in Kamchatka for tephrochronology (Braitseva et al., 1997). Additionally, two Pleistocene caldera-forming episodes occurred, the oldest at 162 ka (see below). All the calderas of Ksudach Volcano are morphologically well preserved (Fig. 5), as is the stratigraphy of intracaldera domes and lavas (Table 3). The evolutionary pattern of Ksudach Volcano can thus serve as a model for older, more obscured calderas in Kamchatka. Geomorphological evidence suggests that Ksudach Volcano was glaciated during the Pleistocene and that interglacial lakes likely filled its calderas. A sudden outburst of post-glacial meltwaters during the Holocene created Teplaya River Canyon to the north (Fig. 5), exposing lavas of the old volcanic edifice.

This work constrains the age of the oldest Pleistocene caldera to 162 ± 17 ka using an ignimbrite outcrop located near the caldera rim (sample 11 M-2002, Fig. 5). The diameter of this caldera is roughly 9 km. This dacitic ignimbrite likely represents the largest caldera-forming eruption of Ksudach Volcano because its caldera boundary encloses all subsequent calderas. Younger Pleistocene pumices (samples 02IPE-15,16, Table 3), thought to represent another episode of caldera formation did not return meaningful Ar–Ar ages.

Notably, all the silicic rocks of Ksudach Volcano are low-$\delta^{18}O$ magmas that help fingerprint eruptive products of Ksudach Volcano (Fig. 6). The 162 ka ignimbrite, however, displays normal-$\delta^{18}O_{melt}$ values of 5.97‰, higher than any younger eruptive products. New Sr isotope analyses of this ignimbrite reveal that it is the least radiogenic among subsequent units, with a $^{87}Sr/^{86}Sr$ value of 0.703298 (Table 3).

Compositionally, caldera formations at Ksudach are associated with the cyclic evolution of magma composition through time, which oscillated between silicic andesites and rhyodacites (Volynets et al., 1999). Our investigation of Pleistocene ignimbrites extends this record to two older caldera-forming episodes (samples 11 M-2002/2, and 02IPE-15,16, Table 3). Furthermore, caldera-forming eruptions KS_3 and KS_4 are zoned, with more evolved rhyodacitic material erupting in the beginning of each eruption, which suggests a zoned magma reservoir of several km^3 in volume and that each eruption caused draw-down to a bottom portion of this reservoir. Olivine–anorthite cumulate inclusions common in Kamchatka (Bindeman and Bailey, 1999) are abundant in many Ksudach Volcano products, especially in KS_2. These cumulates record low-$\delta^{18}O_{melt}$ values (5.2‰, Fig. 5b), suggesting their genetic relationship to the parental magma.

The most dramatic caldera-forming episode is related to the KS_1 eruption of 18–19 km^3 of rhyodacite, the most compositionally-evolved rock at Ksudach Volcano. This eruption, the largest in Kamchatka during the past 2000 years (Braitseva et al., 1996), likely tapped an evolved rhyodacitic reservoir. Following this large eruption, which likely evacuated the entire silicic reservoir, intracaldera volcanic activity resulted in formation of the post-caldera Stübel Cone, which erupted more mafic rocks in the beginning. Some later eruptions from the Stübel Cone, including one in 1907 AD, delivered ~1 km^3 of dacitic tephra signifying new differentiating episode (Volynets et al., 1999).

All the Ksudach magmas belong to the same subalkaline, low-K evolution trend that is common to the EVF magmas of Kamchatka. The earliest stages of Ksudach Volcano, prior to its first caldera-forming eruption at ca 162 ky, were represented by mafic magmas, one of which (02IPE-49) was dated with large error at 324 ± 160 ky (Table 3). These lavas and the early basaltic cinder cones of post KS5 age (Table 3) have similar Sr and Nd isotope compositions while the neighboring stratocone of Zheltaya mountain has higher Sr and lower Nd values. It is thus likely that for several thousand years prior to 162 ky, a volcano of largely basaltic composition existed at the current location of Ksudach Volcano (e.g. Selyangin, 1990).

New Ar–Ar and ^{14}C geochronology demonstrate an interesting evolution pattern for the last 162 ky (Fig. 6a,b). Lavas and smaller-volume pyroclastic units belonging to the pre-1800 BP sequence form a temporal array of decreasing $\delta^{18}O$ values and increasing Sr isotopic values in phenocrysts. Oxygen isotope values in Holocene melts from Ksudach Volcano decrease from 5.4 to 4.7‰ while Sr isotope values increase from 0.70331 to 0.70338 and Sr and O isotopes are anti-correlated (Fig. 6). Products of the earliest caldera-forming eruption at 162 ky, precaldera mafic magmas and the extracaldera Zheltaya Mt deposits, have normal $\delta^{18}O$ values (5.8‰) that are similar to other volcanoes in the EVF (Table 3; Bindeman et al., 2004; Duggen et al., 2007). At the same time, the youngest, most evolved, and most voluminous products of KS_1 are most depleted in $\delta^{18}O$ values and have the highest $^{87}Sr/^{86}Sr$ values. After the early portion of the KS_1 eruption, lavas regain more normal $\delta^{18}O$ values and have lower $^{87}Sr/^{86}Sr$ values. Nd isotopes do not show any temporal trend.

Electron microprobe investigation of minerals in products of the caldera-forming eruptions (Fig. 7) demonstrates concurrent evolution of phenocrysts, with plagioclase becoming more sodic and pyroxene phenocrysts getting more Fe-rich at younger ages, reaching the most evolved values in KS_1. Fe–Ti oxides demonstrate a trend of decreasing temperatures and increasing oxygen fugacity at younger ages, with

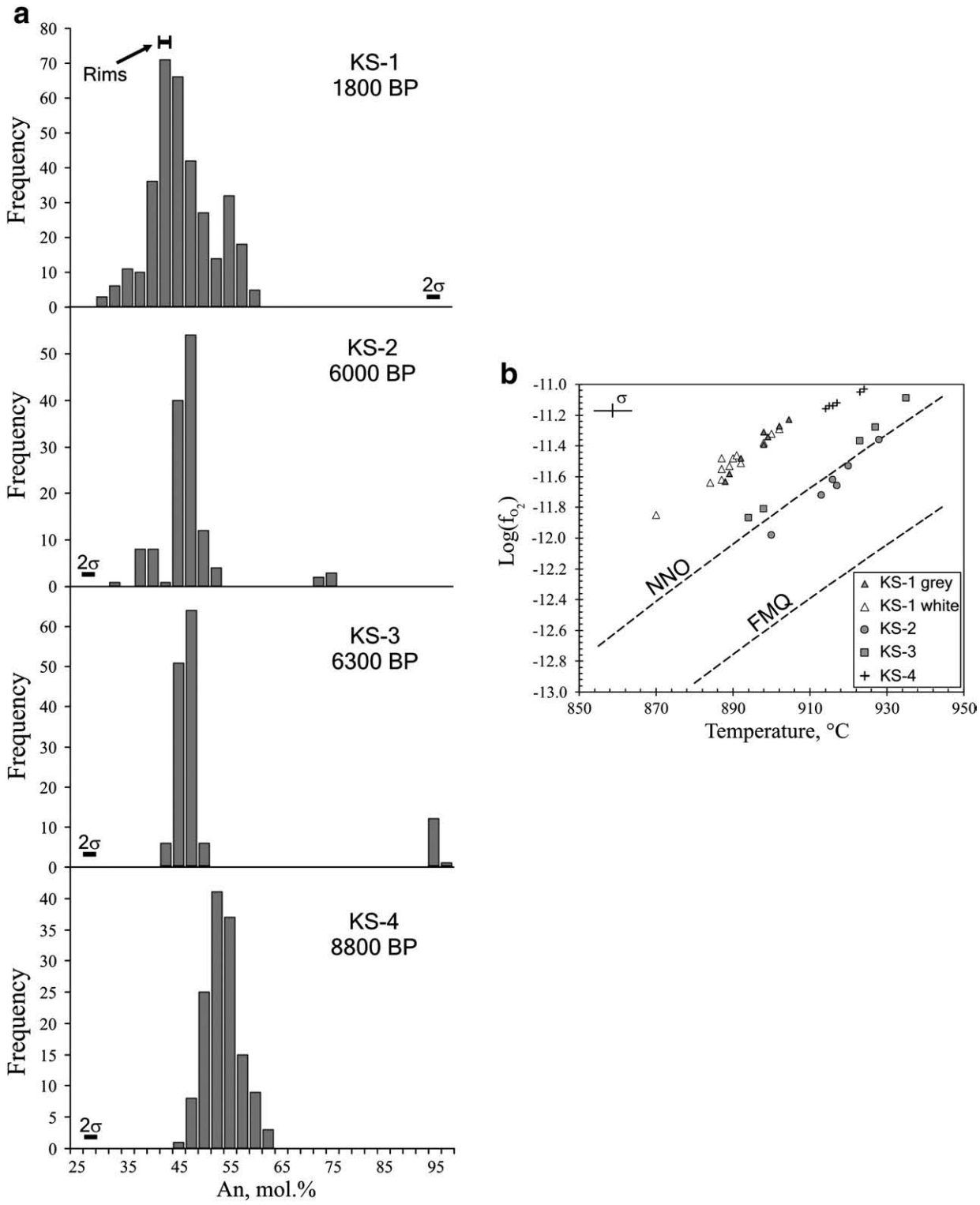

Fig. 7. Evolution of minerals in products of caldera-forming eruptions of Ksudach. a) Plagioclase becomes more sodic with time, suggesting a continuously differentiating single magma reservoir that is getting periodically tapped by small scale caldera formations. b) Fe–Ti oxides in products of caldera-forming eruptions of Ksudach; KS1 taps the most oxidized, thermally-zoned reservoir.

KS_1 tapping the most oxidized, thermally-zoned reservoir (Fig. 7b). Phase equilibria experiments on the KS_1 composition suggest shallow (1.0 kbar) pre-eruptive storage conditions for the products of the 1800 BP KS_1 caldera-forming eruption (Izbekov et al., 2003; Andrews, 2009).

Patterns of compositional and isotopic evolution over time for Ksudach Volcano suggest the following model for its evolution. Initially, a large basaltic volcano (e.g. Selyangin, 1990) developed its first known silicic magma, which erupted in the course of caldera formation 162 ka yielding normal-$\delta^{18}O$ magmas. Since then, whole-rock and mineral compositional trends indicate periodic basaltic magma refills, differentiation, and magma mixing in shallow magma chambers between caldera-forming episodes. In addition to the important role of fractional crystallization, oxygen isotopic trends

and Sr isotopes (Fig. 6a,b) suggest that assimilation and melting of low-$\delta^{18}O$ hydrothermally-altered carapace around this magma body played an important role in explaining magma diversity and the predominance of silicic rocks in the later evolution of Ksudach Volcano. The fact that the 162 ka caldera-forming ignimbrite is normal-$\delta^{18}O$, and that other volcanoes nearby, in particular the closest, Zheltaya Mt, are normal $\delta^{18}O$, rules out that the low-$\delta^{18}O$ anomaly at Ksudach Volcano is of mantle origin. Subsequent caldera collapses transported hydrothermally-altered low-$\delta^{18}O$ intracaldera rocks vertically downwards towards the magma chamber where assimilation of these buried, hydrothermally-altered Ksudach rocks caused progressively lower $\delta^{18}O$ with each new caldera collapse cycle. The rhyodacites of the youngest, most voluminous, and likely the shallowest KS_1 caldera-forming eruption are the most depleted, requiring a composition of 15% hydrothermally-altered crust in magma products.

Low-$\delta^{18}O$ values, shallow storage pressures of 1 kb, and temporal isotopic trends imply that at least 18–19 km^3 of siliceous magma was stored in the very shallow (~3 km, Izbekov et al., 2003; Izbekov, unpublished data) crust prior to the 1800 BP KS_1 eruption for several thousand years after the previous eruption. Because the trend of $\delta^{18}O$ depletion is continuous while Sr and Nd isotopes quickly returned to pre-caldera values, it appears that older and smaller episodes of caldera-forming eruption failed to exhaust the low-$\delta^{18}O$, high $^{87}Sr/^{86}Sr$ components (magma + cumulates) completely and these components accumulated in the upper crustal magma generation zones. Temporal isotopic trends suggest that the dominant petrogenetic process for thousands of years before the 1800 BP eruption was progressive assimilation–remelting of the hydrothermally-altered predecessors driven by the heat of crystallizing basaltic magma.

The pre-1800 BP KS_1 large magma body became the most $\delta^{18}O$ depleted, but it was also the most water saturated and oxidized of all the KS eruptions (Fig. 6d, Izbekov et al., 2003). We speculate that the water inherited from assimilation of shallow, hydrothermally-altered roof-rocks contributed to oxidation. At 1800 BP, a large caldera-forming eruption of KS_1 emptied the entire low $\delta^{18}O$ magma chamber signifying the end of the Pleistocene–Holocene magma body that had persisted for thousands of years. An alternate hypothesis is that the active system moved downward because of freezing of the shallow system, but this is less likely because the KS_1 phase experiments indicate a shallowest (1 kb) equilibration pressure (Izbekov et al., 2003). Finally, eruptive degassing of the massive KS_1 eruption could have caused the remaining KS_1 magma to solidify.

The youngest (post 1800 BP) products of the post-KS_1, are represented by the intracaldera Stübel Cone that have more normal, yet diverse, $\delta^{18}O$ and $^{87}Sr/^{86}Sr$ values, signifying a fundamentally new cycle of magmatic activity involving fresh basalt that was able to get through the evacuated and solidified KS_1 magma chamber. These basalts and more differentiated products have evidence of isotopic mixing with the leftover products of the KS_1 chamber.

Since lowering of the $\delta^{18}O$ value from background, mantle-like values to the observed low-$\delta^{18}O$ values has taken place over a period of ~160 ky, Ksudach Volcano is an ideal example for comparison to identify other calderas in Kamchatka. After the initial caldera formation, a new meteoric–hydrothermal center was established and volcanic cannibalization of hydrothermally-altered rocks during overlapping caldera collapses contributed progressively more low-$\delta^{18}O$ material into the younger magmas.

4.4. Other large calderas of the Eastern Volcanic Front

Most other calderas in the EVF belong to the Central Volcanic Zone (Fig. 2) from the Karymsky Caldera Center in the south to Plateau Zheleznodorozhnoye (Railroad Plateau) in the north. Their caldera sizes, thicknesses of proximal ignimbrite sheets, chemical and isotopic parameters, and newly-determined ages are given in Tables 1 and 2. It is worth noting that oxygen isotopic values of ignimbrites vary dramatically among these calderas and span the entire range for Kamchatkan volcanic products determined earlier (Bindeman et al., 2004), permitting isotopic fingerprinting of eruptive products from different caldera complexes. The EVF was glaciated during the Pleistocene. Below we discuss each volcanic center in the EVF and provide a synthesis of available geologic data from the authors of this paper and their colleagues.

4.4.1. Stol Mountain

This is the oldest known ignimbrite and is densely welded and nearly aphyric andesitic in composition, an outcrop of which is located to the west of the presently active EVF and occurring stratigraphically below a thick layer of basaltic lava, which presumably corresponds to that underlying most of the volcanic edifices in the EVF (Shantser and Krayevaya, 1980). The ages of these basalts were estimated at 3 to 1 Ma (Kozhemyaka et al., 1987). The Stol Mt Ignimbrite yielded an age of 3.71 ± 0.08 Ma (sample 2007B-6), contained low-K values indicative of being derived from the EVF, and high-$\delta^{18}O$ values (7.2‰). The existence of the Stol Mt Ignimbrite thus contradicts the present belief that volcanism in the EVF started in the Plio-Pleistocene with the eruption of basalts and finished with the eruption of silicic rocks that formed caldera centers in the Late Pleistocene. While the regional eruption of plateau basalts across Kamchatka in the Early Pleistocene may record intra-arc tectonic extension (Volynets et al., 1992), the Stol Mt Ignimbrite may represent the little known silicic counterpart of this process and the end of the previous basaltic–silicic cycle in eastern Kamchatka. Stol Mt. deposits sample rather similar stratigraphy of the EVF: 1) >200 m of conglomerate at the bottom (depression fill?); 2) mega-plagioclase rich basaltic lavas followed by silicic ignimbrites; 3) lake deposits; and 4) olivine basalts at the top.

4.4.2. Karymsky Caldera Center

Several large calderas are associated with the Karymsky Caldera Center (Fig. 2), which has overall dimensions of 55 × 65 km, and a total volume of exposed erupted material (younger than 3 Ma) of 1700 km^3. The total volume of silicic ignimbrites is estimated to be 280 km^3 (Masurenkov, 1980; Fedotov and Masurenkov, 1991). In the first half of the exposed Late Pliocene–Early Pleistocene volcanic record, volcanism was largely basaltic and is represented by plateau basalts, similar to those at Stol Mt.

The eastern portion of the oldest known ignimbrite east of the Karymsky Caldera Center, dated as 1.26 ± 0.01 Ma (sample 509-1), is exposed along the Korneva River Valley. This ignimbrite is closely associated in time and space with similar ignimbrites, which have outcrops located in the banks of the neighboring Karymskaya and Zhupanova Rivers. Both exhibit similar zoning from densely welded ignimbrites that are continuously but sharply overlain by less welded ignimbrites with obsidianic fiamme and then by poorly sorted pumices. The estimated aerial extent of exposed remnants of these ignimbrite sheets, is 70–80 km^2. The dated dacitic ignimbrites are exposed at sites 45 m high in the hills on the eastern side of the Karymsky Caldera Center, and exhibit low-$\delta^{18}O$ magma values (4.6‰). The source caldera for the Korneva River Ignimbrites is debated. One coauthor (Bazanova) considers that the source caldera is not preserved and is most likely completely filled with younger volcanics in the region of the Upper Karymsky River and the surrounding territory presently occupied by the younger Stena–Soboliny and Polovinka Calderas. However, another coauthor (Leonov) considers these ignimbrites analogous to the Stena–Soboliny ignimbrites (sample 2007 L-22).

The second regional ignimbrite is associated with the 20 × 10km Stena–Soboliny Caldera in the northwest periphery of the Karymsky Caldera Center. The maximum thickness of this ignimbrite is 200 m and it is present in every direction surrounding the caldera (Fig. 2), which suggests its close association with this caldera. Field studies

indicate that it is likely composed of two to four individual units, which are densely welded at the bottom and more pumiceous at the top, and all are dacitic–andesitic in composition. The lowest flow (sample 2007 L-22) yielded an Ar–Ar in plagioclase age of 1.13 ± 0.1 Ma (Table 1); This dacitic ignimbrite has normal to moderately low-δ^{18}O values of 5.7‰. The youngest flow thought to be associated with Stena–Soboliny Caldera is compositionally zoned from rhyodacitic to dacitic–andesitic and contains no quartz. The time gap between the eruptive events that produced the top and bottom ignimbrites is yet to be determined.

The 11 km-wide Polovinka Caldera, preserved as a fragment on the southern edge of the Karymsky Caldera Center, has yielded an age of 0.432 ± 0.008 Ma (Table 1) from its associated ignmibrite (sample 1999 L-9). Stratigraphically, this ignimbrite lies on top of ignimbrites from the Stena–Soboliny Caldera without an easily visible gap or erosional boundary. However, compositionally and mineralogically, Polovinka Caldera Ignimbites are primarily siliceous: high-silica to low-silica rhyolites with quartz and biotite, which are overlain by pumices of dacitic to andesitic compositions. The studied ignimbrites, located at Pravaya Zhupanova River, have a visible thickness of 100 m and show no evidence of a temporal break between earlier erupted high-silica rhyolites and the dacitic andesites on top. Another dated sample (7 L-27) contains xenocrysts of feldspar and partially fused rocks that yielded a much older (55 Ma) age. The δ^{18}O value of this large-volume ignimbrite is 5.23‰, which is defined as moderately low-δ^{18}O magma.

The small 4 × 6 km Odnoboky Volcano and its associated caldera is entirely enclosed within the Polovinka Caldera (Fig. 2) and yielded an Ar–Ar age of 0.069 ± 0.003 ka (Table 1, sample 2001-L21) that had previously been dated between 0.08 and 0.11 Ma (Masurenkov, 1980). Oxygen isotopes define normal to moderately low-δ^{18}O magmas (5.76‰). The Polovinka Ignimbrites are overlain regionally by thick layers of glacial moraines, which in turn are overlain by ignimbrites from the Odnoboky Caldera. The age of these regional moraines can thus be constrained as being younger than ~0.43 Ma but older than 0.07 Ma, i.e. they can belong anywhere within the second through fourth glacial cycles (e.g. Martinson et al., 1987).

The remaining three calderas of the Karymsky Caldera Center are younger and were dated by fission track in apatite and whole-rock U–Th methods. Akademy Nauk Caldera is 4 km-wide and has an age ranging from 28–48 ka (fission track) and 18–39 ka (U–Th, Masurenkov, 1980). Karymsky Caldera is 5 km-wide and has an age of 7900 BP (^{14}C), while the 7 km-wide Maly Semyachik Caldera is ~15 ka (U–Th) (Masurenkov, 1980). Such young ages for morphologically-preserved calderas and the age of the older caldera agree with observed geologic relations. Debris, ignimbrites, and pumice-pyroclastic flow deposits of the Akademy Nauk Caldera overlie deposits of Odnoboky Volcano, while Maly Semyachik Caldera is enclosed in the Stena–Soboliny Caldera Complex (Fig. 2).

It appears that most magmas that erupted from the Karymsky Caldera Center have had normal to moderately low-δ^{18}O values for at least the past 1.2 Ma. These δ^{18}O values could be used as a fingerprinting tool to distinguish Karymsky Caldera Center ignimbrites from the neigbouring ignimbrites; high-δ^{18}O Bolshoy Semyachik, and lower-δ^{18}O Uzon Ignimbrites.

4.4.3. Bolshoy Semyachik

Large and extensive ignimbrites of Bolshoy Semyachik are found to the west, south and north of its 10 km-wide caldera. They overlay ignimbrites related to the Karymsky center of Stena–Soboliny, but are themselves covered by the youngest ignimbrites from the Uzon center. Thick (up to 250 m) ignimbrite layers next to the caldera have been subdivided into several types. The earliest ones are rhyodacitic and contain quartz and biotite and yielded Ar–Ar age of 0.56 ± 0.045 Ma. These ignimbrites are overlain without visible time break by the more mafic dacitic to andesitic ignimbrites without quartz, which yielded a nearly identical age of 0.524 ± 0.082 Ma. Large estimated volumes of these ignimbrites of 42 km^3 and the Mt Mazama size caldera permits us to relate these ignimbrites to the caldera formation. At least two more smaller-volume ignimbrites, also zoned from more silicic to more mafic from bottom to top lye on top of the dated ignimbrites and have compositional and mineralogical characteristics of the Bolshoy Semiachik area (Leonov and Grib, 2004; Grib and Leonov, 1993a). All Bolshoy Semyachik silicic rocks are high-δ^{18}O (6.5–7‰, Table 1), which distinguishes them from the underlying Stena–Soboliny and overlying Uzon low-δ^{18}O ignimbrites.

4.4.4. Uzon

Ignimbrites associated with 16 × 10 km Uzon–Geyzernaya depression form two separate fields. Ignimbrites of the northern field are believed to be young at ~30 ka based on ^{14}C date near the Kronotsky lake (Florensky, 1984). It is likely that these 30 ka ignimbrites fill river valleys of Left and Right forks of Zhupanova River up to 60 km downstream and are geomorphologically the youngest ignimbrites. This young ignimbrite also filled the river valley along the rim of the Bolshoy Semyachik Caldera. To the south of the caldera, more eroded Uzon Ignimbrites are exposed on the top of Shirokoye plateau, where three ignimbrite flows could be recognized without obvious time breaks. The geochronological sample 90 L-101 belongs to the upper of these ignimbrites and yielded an Ar–Ar age of 0.278 ± 0.017 Ma. It thus appears that the Uzon–Geyzernaya Caldera is a nested complex of at least two superimposed calderas of different age and more mapping/geochronological work is required to distinguish their development. Compositionally the Uzon Ignimbrites belonging to both the northern and southern fields are rhyodacitic to dacitic without quartz. They are clearly distinguished from all other ignimbrites by having the lowest in Kamchatka δ^{18}O magma values of 4.7–5.1‰; post-caldera extrusive domes on the ring fracture and in the center of the caldera are equally ^{18}O depleted (Bindeman et al., 2004).

4.4.5. Plateau Zheleznodorozhnoye

Ignimbrite exposed in the eroded slopes of Zheleznodorozhnoye (aka Railroad) Plateau yielded an age of 1.29 ± 0.01 Ma and normal-δ^{18}O magma values (Sample 1132-1), and are the northernmost ignimbrite in the Eastern volcanic front. This ignimbrite is cropping out in Bogachevka River valley and has total thicknesses of 120–160 m. The internal structure of this ignimbrite unit is quite complex with one to four individual densely welded, 30 m thick cooling units with gradational transition between themselves and non-welded variety with obsidianic bombs and lapilli. The dated ignimbrites are from the lower unit and lie on top of mafic lavas and tuffs of supposedly Pliocene age, and are covered by 100 m thick plateau basalt lavas. The source caldera for these ignimbrites is not known but it has been suggested by Shantser and Krayevaya (1980) that it could be in the region to the north around Mt. Paltsevaya.

4.4.6. Gorely Volcano

Pleistocene caldera-forming eruption of Gorely Volcano ~33 ka BP (Braitseva et al., 1995) created a 13 × 9 km caldera and generated >120 km^3 dacitic ignimbrite (Selyangin and Ponomareva, 1999). We dated the older obsidianic ignimbrite of similar composition that predated the caldera formation (sample 2005 L-19) and that yielded 0.361 ± 0.008 Ma incrementally-heated age for this obsidian. The existence of an older caldera at Gorely was suggested by Melekestsev et al. (1990). Compositionally, dated Gorely Ignimbrites are medium-K and has low-δ^{18}O glass values of 5.05‰, similar to the younger 33 ka ignimbrite suggesting assimilation of low-δ^{18}O country rocks, and petrogenetic evolution pattern reminiscent of multi-caldera Ksudach volcano. Post-caldera Gorely lavas form a shield-like volcano overlying a subglacial tuya pedestal dating back to the Late Pleistocene time,

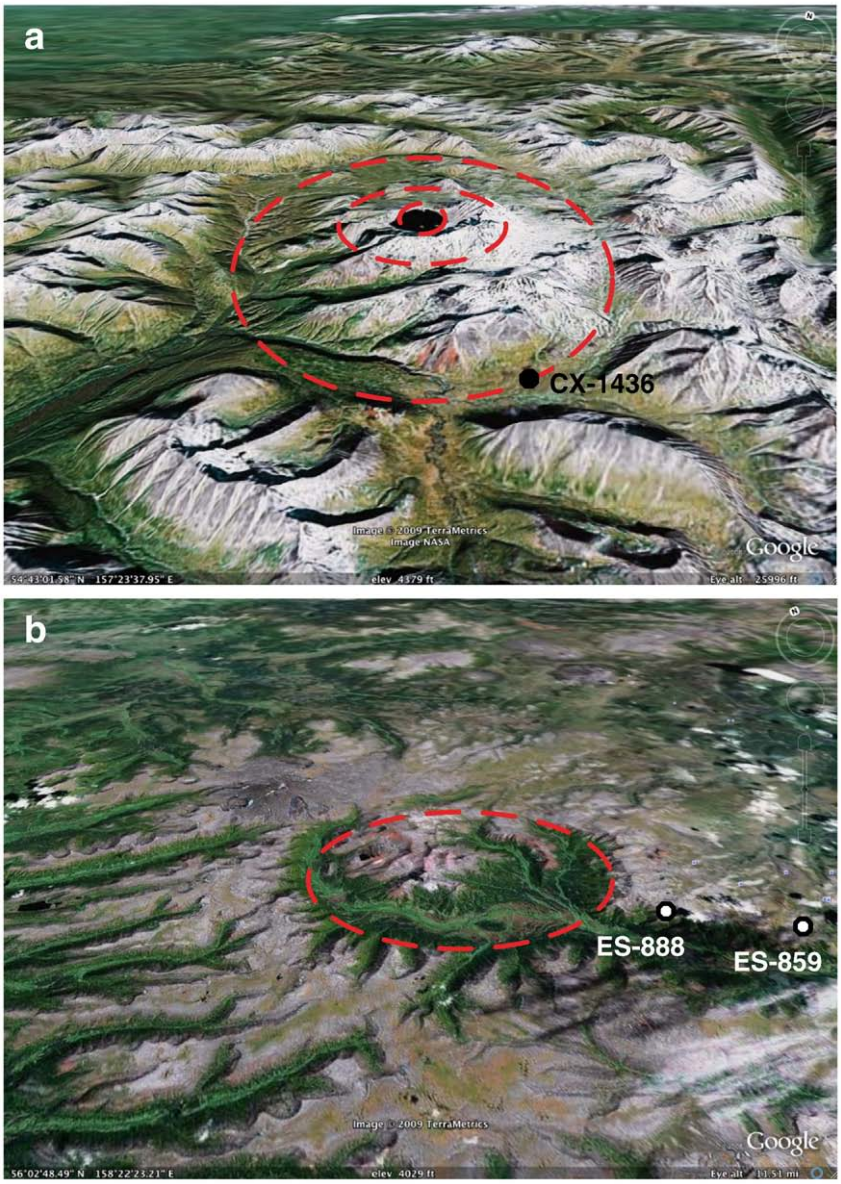

Fig. 8. Aerial view of Khangar (a) and Uksichan Calderas (b) with caldera boundaries and position of dated samples.

when the caldera was filled with ice. Steep, 80–100-m-high slopes of the tuya are still seen in the northern part of the volcanic edifice.

4.5. Major ignimbrites in the Sredinny Range

Volcanism of the Sredinny Range was most active in Pliocene and early Pleistocene when it represented the locus of the volcanic front. Following the accretion of Eastern Peninsula Terrains, the volcanic front rolled back to its present position, while volumes of volcanism in the Sredinny Range significantly diminished (e.g., Lander and Shapiro, 2007). The Sredinny Range is a host for many Pliocene–Pleistocene ignimbrites, four of which are the largest and have been dated in this study: Khangar, Teklentunup, Uksichan, and Noksichan (Fig. 1, Tables 1 and 2).

4.5.1. Khangar Volcano

The volcanic center Khangar is located in the 12×16 km volcano–tectonic depression in the southern part of Sredinny Range and has Paleozoic to Mesozoic gneisses as its basement (Fig. 8a). It had at least two Pleistocene caldera-forming eruptions and a strong explosive eruption in early Holocene (Braitseva et al., 1997; Bazanova and Pevzner, 2001). Tentatively starting in Early Pleistocene, a series of basaltic to andesitic edifices were formed; followed by formation of a large caldera depression measuring 12×16 km in diameter and in this work we dated this earliest ignimbrite of high-silica rhyolitic composition (sample CX-1436) that yielded 0.398 ± 0.008 ka age, thus putting the age of Khangar in Mid Pleistocene. Following the caldera collapse, post-caldera extrusions of dacitic and rhyodacitic composition intruded along the caldera ring fractures. This was followed by another caldera-forming episode that has head to the formation of the caldera 6 km in diameter. Products of this eruption are represented pumice-rich ignimbrites. Volcanic activity in Late Pleistocene was characterized by continuing eruption of dacites and rhyodacites that rebuilt the cone-shaped volcanic edifice, with continuing smaller scale pyroclastic eruptions that are responsible for formation of two smaller craters. The age of two younger caldera-forming eruption has been determined by ^{14}C method at 38–40 ky BP (Braitseva et al., 1995). The last strong eruption 6900 yr BP resulted in

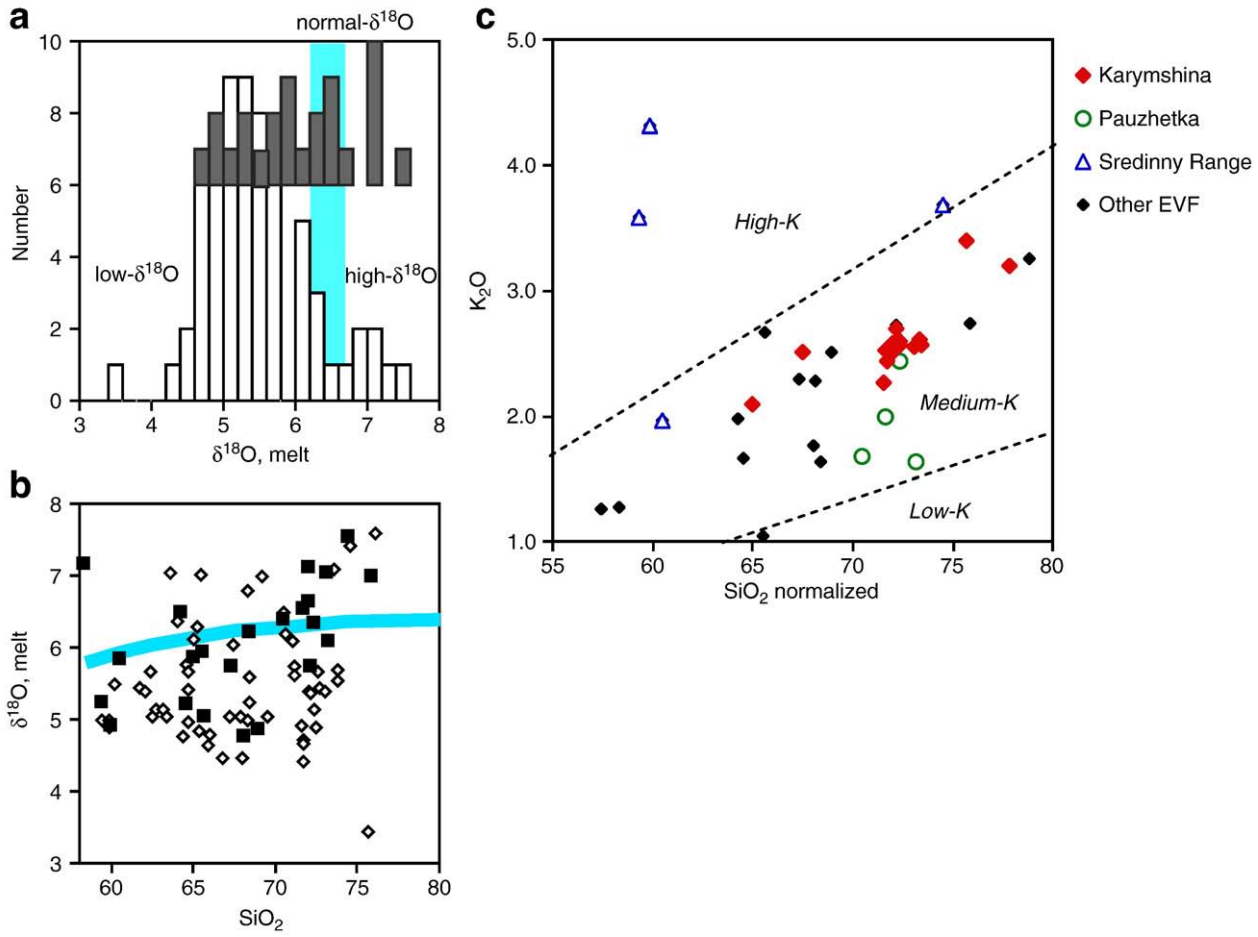

Fig. 9. a) Oxygen isotopic values of large-volume silicic ignimbrites (with few associated lavas) from this study (dark bars or symbols) as compared to the earlier dataset for silicic rocks (Bindeman et al., 2004). Notice that the majority of Kamchatkan lavas represent low-$\delta^{18}O$ magmas. b) $\delta^{18}O$ vs. SiO_2, filled symbols are ignimbrites from this work, open symbols are an earlier dataset for silicic rocks. Line separates low- and vs. normal and high-$\delta^{18}O$ magmas. c) Compositional characteristics of studied samples of large-volume ignimbrites.

formation of the crater with diameter of 3×3.5 km (Bazanova and Pevzner, 2001). The oxygen isotopic values of volcanic products is high-$\delta^{18}O$ with magma values approaching 7.5‰ and easily explained by contamination with metamorphic basement as is also supported by elevated $^{87}Sr/^{86}Sr$ values and the positive variation between the isotopes (Dril et al., 1999). Silicic volcanic products from Khangar are also distinguished by the presence of abundant biotite and amphibole phenocrysts, and moderately high-K values.

4.5.2. Uksichan Volcano

The Uksichan Volcano is among of the largest Pliocene–Quaternary shield edifices with diameter of 48 to 51 km, and a total amount of erupted material of 750 km^3 (Kozhemyaka, 1995). The central part of this edifice contains a large caldera-like depression defined by a series of prominent semi-circular faults. The caldera diameter is 12–13 km, with 900 m depth (Fig. 8b). This caldera culminates the edifice building episodes that had stratovolcano and shield stages, consisting largely of high-K basalts and basaltic andesites at the base, and more differentiated products — shoshonites and latites. The two, closely spaced caldera-forming ignimbrites (ES-888 and ES-859) that we dated at 3.5±0.5 and 3.34±0.07 Ma are represented by latites. They were earlier believed to be of Late Pliocene–Early Pleistocene age. Following the two caldera collapses, a series of extrusive domes of latitic to high-K andesitic composition erupted in the center including the very large extrusions in the center that may represent a resurgent dome. As the Uksichan volcano ceased its existence in Pleistocene, younger basaltic shield volcanoes lye on top of its products.

4.5.3. Nosichan Volcano

The Late Miocene–Early Pliocene Nosichan volcano represents strongly eroded and tectonically fragmented shield volcanic edifice with the base diameter of 12–14 km and total volume of volcanic

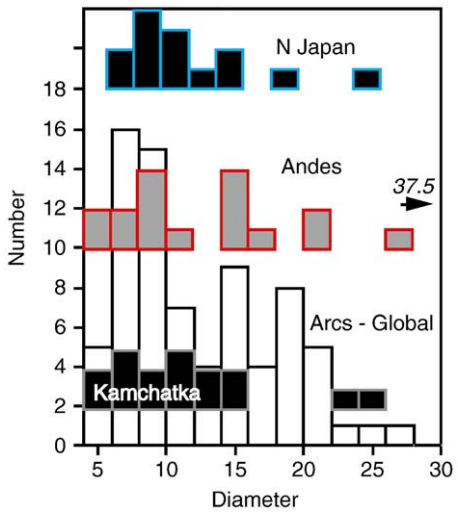

Fig. 10. Diameters of topographically recognizable calderas around the world (Hughes and Mahood, 2008) with Kamchatkan Calderas of this study and calderas in Northern Japan and the Andes.

edifice on the order of 50–60 km^3 that predates the currently active Ichinsky volcano. The shield volcano is made of medium-K basalts, andesites and dacitic lavas. Eruption of 4.02 ± 0.12 Ma (dated sample PP2240) andesitic–dacitic ignimbrites resulted in formation of a caldera depression with estimated diameter of 8 km and depth of 400 m. Following caldera collapse, thick dacitic lava flows on the boundaries of this caldera, as well as dacitic and rhyodacitic extrusions in its central part signifies later stages of silicic volcanism. The eroded edifice of Nosichan is overlain by alkali olivine basalts forming shields and small scoria comes.

4.5.4. Teklentunup Volcano

The Teklentunup Volcano is located in the rear zone of the Sredinny Range and is represented by eroded edifice in Miocene age forming a shield volcano 15–18 km diameter. The total volume of this edifice and associated pyroclastic material are estimated at 80–90 km^3 (Perepelov, 2004, 2005). The latitic ignimbrite dated at 5.7 ± 0.16 Ma (sample TT-7305) represents final stages of evolution of this shield and was formed during collapse of the 6–7 km caldera, with exposed ignimbrites amounting to 8–9 km^3 (Perepelov, 2004, 2005). Following this caldera-forming episode, a stratovolcano filled the caldera and the chemistry of eruptive products became of normal alkalinity. However, a few overlying scoria and small stratocones exhibit wide variations in alkalinity from absarokites to rocks on normal alkalinity. The caldera-forming ignimbrite and post-caldera extrusions are low-δ^{18}O, high-potassium rocks.

5. Compositional and oxygen isotope values of ignimbrites

Major element and oxygen isotopic values of studied Kamchatkan Ignimbrites define wide ranges in SiO_2 and δ^{18}O values (Fig. 9). The new dataset is compared to the earlier dataset of Bindeman et al. (2004), which also includes the many smaller-volume intracaldera units. It is remarkable that more than half of analyzed samples of ignimbrites represent low-δ^{18}O magmas, although the level of depletion is relatively small (<2‰), the volume of studied ignimbrites is significant (hundreds of cubic kilometers). Even 1–2‰ depletion in δ^{18}O requires tens of percent assimilation of, or derivation from low-δ^{18}O hydrothermally-altered crust. In this sense large-volume ignimbrites represent volume-averaged samples of this crust, fingerprinted by low-δ^{18}O meteoric waters acquired during the 2.6 Ma-long Late Quaternary glaciation (e.g. Bindeman et al., 2004).

Compositionally, the majority of ignimbrites are dacitic to rhyodacitic whereas the largest volume ignimbrites of Karymshina and Pauzhetka Calderas are rhyolitic with SiO_2>72 wt.% on a volatile-free basis. Only smaller-volume Karymshina intracaldera extrusions and ignimbrites of Bolshoy Semyachik and Polovinka Calderas are represented by true high-silica rhyolites. K_2O concentration, which is along with SiO_2 is the most diagnostic parameter in distinguishing Kamchatkan tephras (Braitseva et al., 1997), varies expectedly with volcano position relative to the volcanic front. Rocks in the Eastern volcanic front have lower K_2O values, while Sredinny Range volcanics have higher concentrations (Table 2). This trend is characteristic for basalts (Volynets, 1994; Churikova et al., 2001; Duggen et al., 2007) and is inherited by rhyolites.

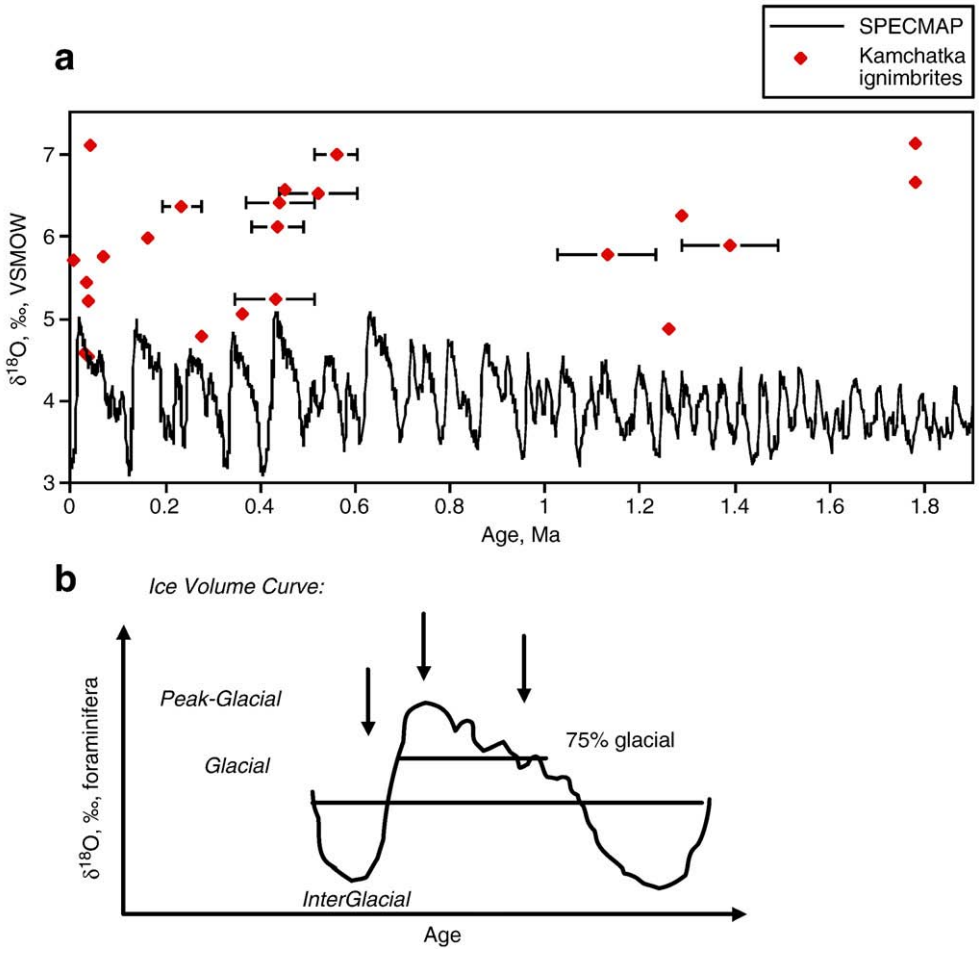

Fig. 11. a) SPECMAP bentic foraminifera that serve as a proxy for global amount of ice and intensity and timing of glacial–interglacial transitions. Superimposed are ages and δ^{18}O magma values of erupted products. The δ^{18}O value of SPECMAP foraminifera is only used as a climate proxy and has no genetic isotopic relation to eruptive products. Notice that the majority (three quarters) of caldera-forming eruptions happened in a period of 75% glacial cover, explained in (b). Oxygen isotopic and age data are from Table 2, while ^{14}C dated Pleistocene caldera-forming eruptions are from Bindeman et al. (2004).

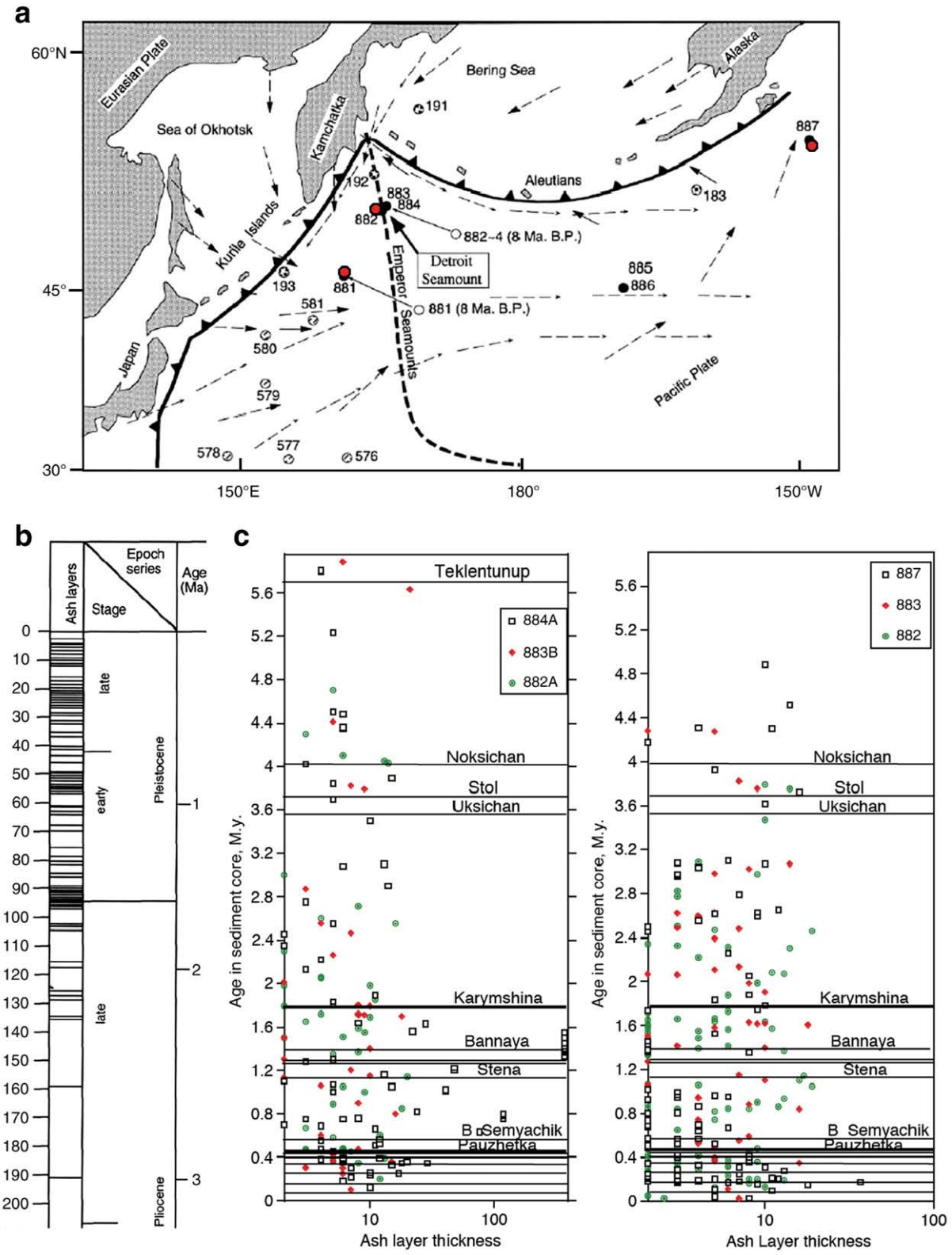

Fig. 12. Submarine ash record off the Pacific coast of Kamchatka. a) Locations of deep sea drilling cores in the vicinity of Kamchatka and the prevailing directions of winds (modified after Cao et al., 1995). b) Distribution of ash layers in hole 884A showing a sudden increase in the number of ash layers starting at ~2.6 Ma. c) Drill cores off-shore of Kamchatka (Prueher and Rea 2001a, right; Cao et al., 1995, left) showing ash layers thicker than 1 cm. Horizontal lines correspond to ages of major caldera-forming eruptions dated in this study. See text for discussion.

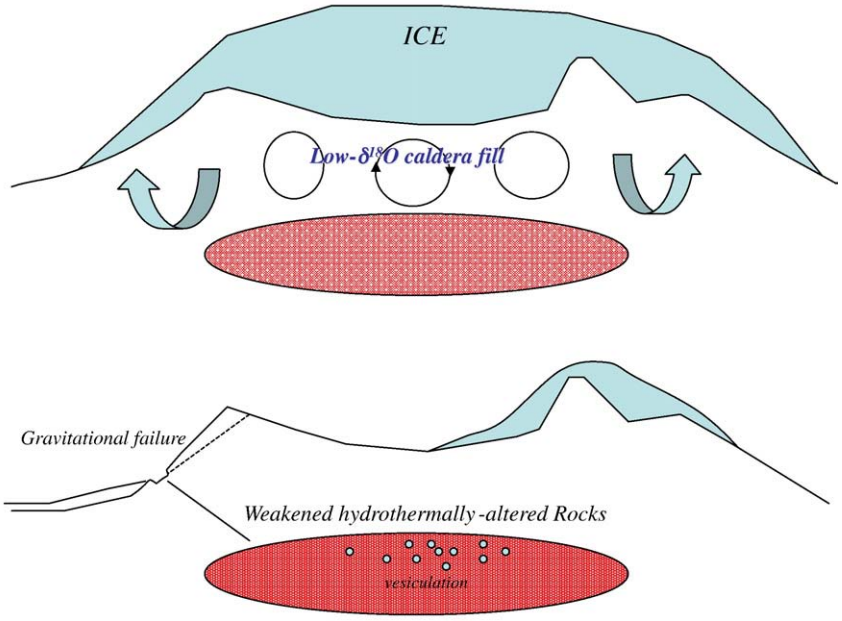

Fig. 13. A cartoon showing glacial–interglacial transition affecting shallow magma chambers and initiating caldera-forming eruptions.

6. Discussion

6.1. Kamchatkan explosive eruptions: how do they rank on a world-wide scale?

The present paper determined the age of the majority of known large-scale caldera-forming episodes in Kamchatka, the significant portion of the Pacific Ring of Fire. Kamchatkan Calderas (and hence volume and magnitude) exceed mapped centers in the neighboring Aleutian and the Kurile arcs, possibly because of thick crust of the Kamchatkan arc, similar to N Japan and the Andes (Fig. 10). A recent compilation by Hughes and Mahood (2008) show that Kamchatka has the highest density of calderas larger than 5 km/1000 km of island arc, for any volcanic arc, and this is likely due to a combination of high arc-perpendicular convergence rate (7–8 cm/yr) and the presence of thick continental crust. Compositionally, Kamchatkan explosive eruptions rank equal to other island arcs with predominance of dacites to rhyodacites among ignimbrites, with lesser abundance of high-silica–rhyolites, the common feature of island arc petrogenesis as compared to intracontinental volcanic provinces, such as Yellowstone. Using the same database of Hughes and Mahood (2008) for other island arcs, and updating the information on caldera sizes and their relative number for Kamchatka based on the results of this paper, we observe that the average caldera size increases with the increase in the inferred crustal thickness in the sequence: Aleutians–Kuriles–N Japan–Kamchatka–Andes (Fig. 10). Average Kamchatkan Caldera sizes are slightly smaller than those in the Andes but the number of caldera-forming eruptions per 1000 km of arc length is significantly larger: 15 (in Kamchatka) vs. 7 (S Andes) or 2–3 (N and Central Andes). This comparison distinguishes Kamchatka as the volcanic arc with the most voluminous explosive output.

6.2. Caldera-forming eruptions and glacial–interglacial transition

Estimates on the extent of glaciation in Kamchatka and NW Asia range from continental (Grosswald, 1998) to alpine (Braitseva et al., 1968). Recent reconstruction of moraine distribution in Kamchatka supports the later view but permits significant glaciers to reach both Pacific and Okhotsk shores (Bigg et al., 2008). Ice rafted debris are abundant in N Pacific (Prueher and Rea, 2001a,b) and iceberg discharge pathways suggest Kamchatkan source at least to 882–884 cores (Bigg et al., 2008). In all reconstructions, all volcanic ranges in the eastern volcanic front and in Sredinny Range were covered by hundreds of meters of ice.

The presented data allow us to put the ages of the eruptions in the context of the global SPECMAP bentic foraminifera $\delta^{18}O$ record (Imbrie et al., 1984; Lisiecki and Raymo, 2005), which serves as a good globally-averaged proxy for climate change in Pliocene and Quaternary. In order to determine if Ar–Ar dates plot in "glacial" or "interglacial" time, we took the age of the eruptions and correlated it with the appropriate glacial cycle. Maximum and minimum $\delta^{18}O$ foraminifera values of this glacial cycle were taken to reflect the full range of climate change during the climate change cycle, and thus position of the eruption closer to the maximum $\delta^{18}O$ value (coldest, glacial time, maximum ice, Fig. 11) or low-$\delta^{18}O$ value (warmest and interglacial) can be estimated for each age of the eruption.

Perhaps the most surprising result of the present study is that out of 16 new ages of large caldera-forming eruptions three quarters plot in the "75% glacial" time. This result gets additional confirmation when we consider an radiocarbon-dated peak of volcanic activity that falls during the youngest glacial maximum near 37–38 ky (Table 1). Furthermore, the positive correlation of glaciation and the number of explosive volcanic eruptions is evident in N Pacific drill cores (Fig. 12; Prueher and Rea, 2001a,b; Cao et al., 1995) off the coast of Kamchatka, which shows sudden increase in glacial deposits and volcanic ash layers starting at about 2.6 Ma (Fig. 12b). The increased explosive volcanic activity in the Quaternary is a known observation in many other drill cores around Pacific and elsewhere (Kennett and Thunell, 1977) and thus this correlation may characterize other glaciated areas in the Aleutians and Alaska that supplied ash to the locations drilled, and the Hole 183 in particular (Fig. 12a).

6.3. Ash record in NW Pacific and glacial–interglacial connection

Records of ash present in drillcores 881–884, 887 of the Ocean Deep Sea Drilling Project were presented by Prueher and Rea (2001a, 2001b) and Cao et al. (1995). The latter work presents exhaustive and highly detailed chemical analysis of a majority of many tens of ash layers including trace elemental and isotopic data. We plotted the stratigraphic sedimentological ages against thicknesses of ash layers over in drill cores 882, 883, and 887 from Prueher and Rea (2001a, 2001b) and 882A, 883A, and 884B from Cao et al. (1995). These are

drill cores in the vicinity of Kamchatka spanning over 5 Ma of sedimentological record (Fig. 12b,c). In particular, glass shards in ash record show oscillating high K_2O and low-K_2O rhyolitic varieties that can be attributed to volcanic eruptions in the Sredinny Range and Eastern Volcanic front respectively (Fig. 1). We also plotted newly-determined ages of studied eruptions in an attempt to find a match of the thickest ash layers with the dated eruptions. This is particularly warranted for two supereruptions that we identified: 1.78 Ma Karymshina and 0.45 Ma Pauzhetka Calderas.

Results of this comparison are rather inconclusive. Not only that is difficult to find identical ash layer of comparable thickness in these neighboring holes, the dated eruptions do not match even within several hundred thousand years. Exceptionally thick ash layers are found in the hole 884B (Cao et al., 1995): 370 cm at 1.3–1.55 Ma, 118 cm at 0.78–0.8 Ma. Should sedimentological ages for these ash layers be corrected, then these two thickest ash layers would correspond to Karymshina and Pauzhetka Caldera-forming eruptions. Compositionally both ash layers are low-K_2O and thus this is permissive, pending better age resolution in the drill cores and/or using the ages of determined eruptions as marker layers in drill cores. Two additional thick ash layers: 41 cm at 1.02 Ma, and 48 cm at 1.21 Ma with K_2O values appropriate for the Eastern Volcanic front may correspond to the Stena–Soboliny and Korneva River ignimbrites.

6.4. What causes explosive eruptions and low-δ18O values during the glacial times?

The observation presented here that the majority of eruptions happened during a maximal ("75% glacial") period is counterintuitive and deserves discussion. There were many attempts to describe periodicity of volcanic eruptions, both basaltic and silicic, explosive and effusive, to external factors varying from sea-level change, tides, to glaciations (Kennett and Thunell, 1977; Rampino et al., 1979; Wallman et al, 1988; Glazner et al., 1999; Gusev et al., 2003; Jellinek et al., 2004; Jicha et al., 2009). It appears that glaciations have documented influences on volcanism in Iceland, Sierra Nevada, and NE Pacific, with increased mantle melting productivity and formation of the crustal magma chambers. However the connection between deglaciation and increased volcanism is not straightforward: melting glaciers (glacial unload) do not automatically cause volcanic eruptions because lithostatic and hydrostatic pressure differential remains the same. Thus, association of the thickest ice with calderas makes them most susceptible to pressure fluctuation during interstadial and deglaciation episodes: caldera walls may experience cone failure during deglaciation (Waythomas and Wallace, 2002; Huggel et al., 2007).

Jellinek et al. (2004) attributed the rate of change — first derivative of δ^{18}O-time forminifera SPECMAP data — as a leading cause of triggering volcanic eruptions. Peaks of basaltic and silicic eruptions in eastern Sierra Nevada (Glazner et al., 1999) demonstrated delay after deglaciation at 3 ka (basaltic) and 11 ka (silicic) eruptions. These delays were explained by the elastic response of the mantle and the crust (Slater et al., 1998; Jellinek et al., 2004).

Our observation that the majority of studied Kamchatkan eruptions happen during glacial times supports this view. Glacial times represent the more dynamic conditions for change, with multiple fluctuation of the amount of ice, while ice-free or ice poor interglacial periods do not cause oscillating pressure over magma chambers (Fig. 13). The other factors that may promote greater explosivity during glacial periods involve specific hydrogeologic conditions for hydrothermal circulation around caldera-covered volcanic centers (Fig. 13). Confined hydrothermal circulation under ice may cause greater weakening of the intracaldera roof rock, formation of structurally-weak and permeable tuyas and hyaloclastites like in Iceland, that are more prone to subsequent collapse in interstadial. This hydrothermal weakening may contribute to catastrophic volcanic edifice failures caused by glacial erosion and deglaciation (e.g. Waythomas and Wallace, 2002). An additional consideration for explosive eruptions happening during glacial periods may be related to increased accumulation of gas phase in their parental magma chamber (Fig. 13), both due to magma chamber saturation with volatiles, and by water inherited from assimilation of the surrounding meteoric–hydrothermal system.

An independent memory of glaciations in erupted volcanic products is delivered by their low-δ^{18}O values, making Kamchatka one of the provinces around the world with abundant low-δ^{18}O magmas. The appearance of low-δ^{18}O signature in magma is related to remelting of hydrothermally-altered rocks altered by low-δ^{18}O snow water, and seasonally-averaged δ^{18}O values of meteoric waters tend to be lower during the glacial, than intergracial times, which (other conditions being the same) should fingerprint the upper crust with lower δ^{18}O values.

It is hard to distinguish which of these factors played the dominant role but the abundant low-δ^{18}O values in volcanic products from Kamchatka (this work and Bindeman et al., 2004) suggest that the assimilation of hydrothermally-altered rocks from adjacent meteoric–hydrothermal systems played an equally-important role, in addition to the physical changes associated with glacial–interglacial pressure oscillations. While availability of water is likely to be similar in glacial vs. interglacial time in wet Kamchatkan climate, it is the lower-δ^{18}O value of glacial precipitation that has greater isotopic leverage to fingerprint the crust, aiding identification of the shallow petrogenetic processes.

Acknowledgements

This research was chiefly supported by NSF grants EAR0537872 and EAR CAREER 0844772 to INB. Partial support for VVP and LIB came from the grants 09-05-00286 and 09-05-00718 from the Russian Foundation for Basic Research and from NSF grant EAR0125787 to Joanne Bourgeois. The ion microprobe facility at UCLA is partly supported by a grant from the Instrumentation and Facilities Program, Division of Earth Sciences, National Science Foundation. Bundes Ministerium für Bildung und Forschung (KALMAR project) to MVP and VV. We thank EN Grib and AN Rogozin for sample donation and help with fieldwork.

References

Andrews, B.J., 2009. Recharge, decompression, and collapse: dynamics of volcanic processes, University of Texas at Austin, PhD dissertation, 264 pages.

Avdeiko, G.P., Savelyev, D.P., Palueva, A.A., Popruzhenko, S.V., 2007. Evolution of the Kurile–Kamchatka volcanic arcs and dynamics of the Kamchatka–Aleutian junction. In: Eichelberger, J., Gordeev, E., Kasahara, M., Izbekov, P., Lees, J. (Eds.), Volcanism and Tectonics of the Kamchatka Peninsula and Adjacent Arcs: American Geophysical Union Geophysical Monograph Series, vol. 172, pp. 37–55.

Bacon, C.R., 1983. Eruptive history of mount Mazama and Crater Lake caldera Cascade Range USA. J. Volcanol. Geotherm. Res. 18, 57–115.

Bigg, G.R., Clark, C.D., Hughes, A.L.C., 2008. A last glacial ice sheet on the Pacific Russian coast and catastrophic change arising from coupled ice–volcanic interaction. Earth. Planet. Sci. Lett. 265, 559–570.

Bindeman, I.N., 2008. Oxygen isotopes in mantle and crustal magmas. In: Putirka, K.D., Tepley, F.J. (Eds.), Reviews in Mineralogy and Geochemistry, vol. 69, pp. 445–478.

Bindeman, I.N., Bailey, J.C., 1994. A model of reverse differentiation at Dikii Greben' Volcano, Kamchatka: progressive basic magma vesiculation in a silicic magma chamber. Contrib. Mineral. Petrol. 117, 263–278.

Bindeman, I.N., Bailey, J.C., 1999. Trace elements in anorthite megacrysts from the Kurile island arc: a window to across-arc geochemical variations in magma compositions. Earth. Planet. Sci. Lett. 169, 209–226.

Bindeman, I.N., Vinogradov, V.I., Valley, J.W., Wooden, J.L., Natal'in, B.A., 2002. Archean protolith and accretion of crust in Kamchatka: SHRIMP dating of zircons from Sredinny and Ganal Massifs. J. Geol. 110, 271–289.

Bindeman, I.N., Ponomareva, V.V., Bailey, J.C., Valley, J.W., 2004. Volcanic arc of Kamchatka: a province with high-delta O-18 magma sources and large-scale O-18/O-16 depletion of the upper crust. Geochim. Cosmochim. Acta 68 (4), 841–865.

Bindeman, I.N., Schmitt, A.K., Valley, J.W., 2006. U–Pb zircon geochronology of silicic tuffs from the Timber Mt/Oasis Valley caldera complex, Nevada: rapid generation of large-volume magmas by shallow-level remelting. Contrib. Mineral. Petrol. 152, 649–665.

Bazanova, L.I., Pevzner, M.M., 2001. Khangar: one more active volcano in Kamchatka. Transactions (Doklady) of the Russian Academy of Sciences. Earth Sci. 377A, 307–310 March–April.
Braitseva, O.A., Melekestsev, I.V., Evteeva, J.S., Lupikina, Y.G., 1968. Stratigraphy of Quaternary deposits and glaciations of Kamchatka. Nauka, Moscow. 226 p.
Braitseva, O.A., Litasova, S.N., Ponomarenko, A.K., 1987. Application of tephrochronological method for dating of the key archaeological site in Eastern Kamchatka. Volcanol. Seismol. 5, 507–514.
Braitseva, O.A., Melekestsev, I.V., Ponomareva, V.V., Sulerzhitsky, L.D., 1995. The ages of calderas, large explosive craters and active volcanoes in the Kuril–Kamchatka region. Russia. Bull. Volcanol. 57 (6), 383–402.
Braitseva, O.A., Melekestsev, I.V., Ponomareva, V.V., Kirianov, V.Y., 1996. The caldera-forming eruption of Ksudach volcano about cal. AD 240, the greatest explosive event of our era in Kamchatka. J. Volcanol. Geotherm. Res. 70, 49–66.
Braitseva, O.A., Ponomareva, V.V., Sulerzhitsky, L.D., Melekestsev, I.V., Bailey, J.C., 1997. Holocene key-marker tephra layers in Kamchatka. Russia. Quat. Res. 47, 125–139.
Cao, L.-Q, Arculus, R.J., McKelvey, B.C., 1995. Geochemistry and petrology of volcanic ashes recovered fron sites 881 through 884: a temporal record of Kamchatka and Kurile volcanism. Proceedings of the Ocean Drilling Program: In: Rea, et al. (Ed.), Scientific Results, vol. 145, pp. 345–381.
Chen, C.H., Shieh, Y.N., Lee, T., Chen, C.H., Mertzman, S.A., 1990. Nd–Sr–O isotopic evidence for source contamination and unusual mantle component under Luzon Arc. Geochim. Cosmochim. Acta 54, 2473–2484.
Chen, C.H., DePaolo, D.J., Nakada, S., Shieh, Y.N., 1993. Relationship between eruption volume and neodymium isotopic composition at Unzen volcano. Nature 362, 831–834.
Churikova, T., Dorendorf, F., Worner, G., 2001. Sources and fluids in the mantle wedge below Kamchatka, evidence for across-arc geochemical variation. J. Petrol. 42, 1567–1593.
Dril, S.I., Pokrovsky, B.G., Perepelov, A.B., Baluyev, E.Y., Bankovskaya, E.V., 1999. Khangar Volcano (Kamchatka): $^{87}Sr/^{86}Sr$–$\delta^{18}O$ isotope systematics and genesis of lavas. Proceedings of the International Conference on Isotope Geochemistry, Moscow. p. 124.
Duggen, S., Portnyagin, M., Baker, J., Ulfbeck, D., Hoernle, K., Garbe-Schonberg, D., Grassineau, N., 2007. Drastic shift in lava geochemistry in the volcanic-front to rear-arc region of the Southern Kamchatkan subduction zone: evidence for the transition from slab surface dehydration to sediment melting. Geochim. Cosmochim. Acta 71, 452–480.
Erlich, E., 1986. Geology of the calderas of Kamchatka and Kurile islands with comparison to calderas of Japan and the Aleutians, Alaska. USGS Open File Report vol. 86–291, 300p.
Erlich, E.N., Melekestsev, I.V., Tarakanovsky, A.A., Zubin, M.I., 1972. Quaternary calderas Kamchatka. Bull. Volcanol. 36–1, 222–237.
Fedotov, S.A., Masurenkov, Yu.P. (Eds), 1991. Active volcanoes of Kamchatka. Nauka, Moscow. Vol.1, 302 p. Vol.2, 415 p.
Florensky, I.V., 1984. On the ages of Uzon and Krashenninnikov calderas. Volcanol. Seismol. N1, 102–106.
Florensky, I.V., Trifonov, V.G., 1985. Neotectonics and volcanism in the East Kamchatka volcanic zone. Geotektonika 4, 78–87 [In Russian].
Geist, E.L., Vallier, T.L., Scholl, D.W., 1994. Origin, transport and emplacement of an exotic island arc terrane exposed in eastern Kamchatka. Russia. Geol. Soc. Am. Bull. 106, 1182–1194.
Geyer, A., Marti, J., 2008. The new worldwide collapse caldera database (CCDB.: a tool for studying and understanding caldera processes). J. Volcanol. Geotherm. Res. 175, 334–354.
Glazner, A.F., Manley, C.R., Marron, J.S., Rojstaczer, S., 1999. Fire or ice: anticorrelation of volcanism and glaciation in California over the past 800,000 years. Geophys. Res. Lett. 26, 1759–1762.
Grib, E.N., Leonov, V.L., 1993a. Ignimbrites of the Bolshoi Semiachik caldera, Kamchatka: composition, structure and origin. Volcanol. Seismol. 14 (5), 532–550.
Grib, E.N., Leonov, V.L., 1993b. Ignimbrites of Uzon–Geyzernaya volcano–tectonic depression, Kamchatka: correlation of sections, compositions and conditions of formation. Volcanol. Seismol. 5, 15–33.
Grosswald, M.G., 1998. Late-Weichselian ice sheets in Arctic and Pacific Siberia. Quaternary Int. 45, 3–18.
Gusev, A.A., Ponomareva, V.V., Braitseva, O.A., Melekestsev, I.V., Sulerzhitsky, L.D., 2003. Great explosive eruptions on Kamchatka during the last 10,000 years: self-similar irregularity of the output of volcanic products. J. Geophys. Res. 108/ B2, 2126. doi:10.1029/2001JB000312.
Huggel, C., Caplan-Auerbach, J., Waythomas, C.F., Wessels, R.L., 2007. Monitoring and modeling ice–rock avalanches from ice-capped volcanoes: a case study of frequent large avalanches on Iliamna Volcano. Alaska. J. Volcanol. Geotherm. Res. 168, 114–136.
Hughes, G.R., Mahood, G.A., 2008. Tectonic controls on the nature of large silicic calderas in volcanic arcs. Geology 36, 627–630.
Imbrie, J., et al., 1984. The orbital theory of Pleistocene climate: support from a revised chronology of the marine d18O record. In: Berger, A.L., et al. (Ed.), Milankovitch and Climate, Part 1. Dordrecht, Reidel, p. 269.
Izbekov, P., Gardner, J.E., Andrews, B., Ponomareva, V.V., Melekestsev, I.V., 2003. Petrology of Holocene Caldera-Forming Eruptions at Ksudach, Kamchatka. Eos Trans. AGU, 84(46), Fall Meet. Suppl., Abstract V42B-0347.
Jellinek, A.M., Manga, M., Saar, M.O., 2004. Did melting glaciers cause volcanic eruptions in eastern California? Probing the mechanics of dike formation. J. Geophys. Res. Solid Earth 109 Article Number: B09206.
Jicha, B.R., Singer, B.S., 2006. Volcanic history and magmatic evolution of Seguam Island, Aleutian Island arc. Alaska. Geol Soc. Am. Bull. 118, 805–822.
Jicha, B.R., Scholl, D.W., Rea, D.K., 2009. Circum-Pacific arc flare-up and global cooling near Eocene–Oligocene boundary. Geology art G25392.
Kennett, J.P., Thunell, R.C., 1977. Explosive Cenozoic volcanism and climatic implications. Science 196, 1231–1234.
Konstantinovskaia, E.A., 2001. Geodynamics of an Early Eocene arc-continent collision reconstructed from the Kamchatka Orogenic Belt, NE Russia. Tectonophysics 325, 87–105.
Kozhemyaka, N.N., 1995. Long-living volcanic centers of Kamchatka: types of edifices, duration of existence, volume of volcanic rocks, productivity, balance of magmatism, tectonic position. Volcanol. Seismol. 6, 3–19.
Kozhemyaka, N.N., Ogorodov, N.V., 1977. Some features of volcanism and genesis of Pauzhetka volcano–tectonic depression (Southern Kamchatka). Bulletin Vulkanologicheskikh Stantsii 53, 92–101.
Kozhemyaka, N.N., Litasov, N.E., 1980. Quaternary pumice, tuff and ignimbrite fields and eruptive centers. Long-lived Center of Endogenic Activity in Southern Kamchatka. M. Nauka Press, pp. 116–128. in Russian.
Kozhemyaka, N.N., Litasov, N.E., Vazheyevskaya, A.A., Pampura, V.D., Antipin, V.S., Perepelov, A.B., 1987. Geological strtucture, volcanism and evolution of magmas if Kronotsky-Gamchen structure in Kamchatka. Volcanol. Seismol. 3, 31–50.
Lander, A.V., Shapiro, M.N., 2007. The Origin of the modern Kamchatka zone. Volcanism and Subduction: the Kamchatka Region: Geophys. Monograph Series, vol. 172, pp. 57–64. AGU.
Leonov, V.L., 1989. Structural Conditions of Localization of High-Temperature Hydrothermal Deposits. Nauka publisher, Moscow. [in Russian], available at http://www.kscnet.ru/ivs/monograph/monleon/index.html.
Leonov, V.L., Grib, E.N., 2004. The structural position and volcanism of the quaternary calderas, Kamchatka Russia. Monograph.Vladivostok. Dalnauka publisher. in Russian.
Leonov, V.L., Rogozin, A.N., 2007. Karymchina — gigantic caldera–supervolcano in Kamchatka: boundaries, structure, conditions of formation. Volcanol. Seismol. N5, 14–28 in Russian.
Lisiecki, L.E, Raymo, M.E., 2005. A Pliocene–Pleistocene stack of 57 globally distributed benthic delta O-18 records. Paleoceanography 20, 1 Article number PA1003.
Lonshakov, E.A., 1979. Rows of volcano–tectonic structures and structural matter paragenesis of the Southern Kamchatka region. Bull. Volc. Stantsii 57, 79–91 in Russian.
Martinson, D.G., Pisias, N.G., Hays, J.D., Imbrie, J., Moore, T.C., Shackleton, N.J., 1987. Age dating and the orbital theory of the ice ages: development of a high-resolution 0 to 300,000-year chronostratigraphy. Quat. Res. 27, 1–30.
Masurenkov, Yu.P. (Ed.), 1980. Volcanic Center, Structure, Dynamics, and Erupted Material (Karymsky Structure). Nauka press, Moscow. In Russian.
Melekestsev, I.V., Braitseva, O.A., Erlich, E.N., Kozhemyaka, N.N., 1974. Volcanic mountains and plains. In: Luchitsky, I.V. (Ed.), Kamchatka, Kurile and Commander Islands. Nauka, Moscow, pp. 162–234. In Russian.
Melekestsev, I.V., 1980. Volcanism and Relief Formation. Nauka, Moscow (in Russian).
Melekestsev, I.V., Braitseva, O.A., Ponomareva, V.V., 1990. Holocene activity dynamics of Mutnovskii and Gorelyi volcanoes and the volcanic risk for adjacent areas (as indicated by tephrochronology studies). Volcanol. Seismol. 9/3, 337–362.
Paces, J.B., Miller, J.D., 1993. Precise U–Pb ages of Duluth Complex and related mafic intrusions northeastern Minnesota; geochronological insights to physical petrogenetic paleomagnetic and tectonomagnetic processes associated with the 11 Ga midcontinent rift system. J. Geophys. Res. 98, 13997–14013.
Perepelov, A.B., 2004. Neogene–Quaternary shoshonite–latite magmatism of the Sredinny Range of Kamchatka: Teklentunup volcano (geologic evolution, petrography, mineralogy). Volcanol. Seismol. 3, 12–30.
Perepelov, A.B., 2005. Neogene–Quaternary shoshonite–latite magmatism of the Sredinny Range of Kamchatka: Teklentunup volcano (geochemistry, petrology, geodynamic position). Volcanol. Seismol. 1, 22–36.
Pokrovsky, B.G., Volynets, O.N., 1999. Oxygen–isotope geochemistry in volcanic rocks of the Kurile–Kamchatka arc. Petrology 7, 227–251.
Ponomareva, V.V., Kyle, P.R., Melekestsev, I.V., Rinkleff, P.G., Dirksen, O.V., Sulerzhitsky, L.D., Zaretskaia, N.E., Rourke, R., 2004. The 7600 (^{14}C) year BP Kurile Lake caldera-forming eruption, Kamchatka, Russia: stratigraphy and field relationships. J. Volcanol. Geotherm. Res. 136, 199–222.
Ponomareva, V.V., Churikova, T.G., Melekestsev, I.V., Braitseva, O.A., Pevzner, M.M., Sulerzhitsk, y L.D., 2007a. Late Pleistocene–Holocene volcanism on the Kamchatka Peninsula, Northwest Pacific region. In: Eichelberger, J., Gordeev, E., Kasahara, M., Izbekov, P., Lees, J. (Eds.), Volcanism and Tectonics of the Kamchatka Peninsula and Adjacent Arcs: American Geophysical Union Geophysical Monograph Series, vol. 172, pp. 165–198.
Ponomareva, V.V., Kyle, P.R., Pevzner, M.M., Sulerzhitsky, L.D., Hartman, M., 2007b. Holocene eruptive history of Shiveluch volcano. Kamchatka Peninsula. In: Eichelberger, J., Gordeev, E., Kasahara, M., Izbekov, P., Lees, J. (Eds.), Volcanism and Tectonics of the Kamchatka Peninsula and Adjacent Arcs: American Geophysical Union Geophysical Monograph Series, vol. 172, pp. 263–282.
Portnyagin, M., Hoernle, K., Plechov, P., Mironov, M., Khubunaya, S., 2007. Constraints on mantle melting and composition and nature of slab components in volcanic arcs from volatiles (H2O, S, Cl, F) and trace element in melt inclusions from Kamchatka Arc. Earth Planet. Sci. Lett. 255, 53–69.
Prueher, L.M., Rea, D.K., 2001a. Tephrochronology of the Kamchatka–Kurile and Aleutian arcs: evidence for volcanic episodicity. J. Volcanol. Geotherm. Res. 106, 67–84.
Prueher, L.M., Rea, D.K., 2001b. Volcanic triggering of late Pliocene glaciation: evidence from the flux of volcanic glass and ice-rafted debris to the North Pacific Ocean. Palaegeogr. Palaeoclimat. Palaeoecol. 173 (3–4), 215–230.
Rampino, M.R., Self, S., Fairbridge, R.W., 1979. Can rapid climatic change cause volcanic eruptions? Science 206, 826–829.

Reid, M.R., 2003. Timescales of magma transfer and storage in the crust. In: Rudnick, RL (Ed.), The Crust, Treatise on Geochemistry, Vol. 3. Elsevier, Oxford, UK, pp. 167–193.
Reid, M.R., Coath, C.D., Harrison, T.M., McKeegan, K.D., 1997. Prolonged residence times for the youngest rhyolites associated with Long Valley Caldera: ^{230}Th–^{238}U ion microprobe dating of young zircons. Earth Planet. Sci. Lett. 150 (1–2), 27–39.
Selyangin, O.B., 1990. Geologic structure and evolution of calderas of Ksudach volcano. Volcanol. Seismol. 9 (5), 690–713.
Selyangin, O.B., Ponomareva, V.V., 1999. Gorely volcanic center, South Kamchatka: structure and evolution. Volcanol. Seismol. 21, 163–194.
Schärer, U., 1984. The effect of initial 230Th disequilibrium on young U–Pb ages: the Makalu case Himalaya. Earth Planet. Sci. Lett. 67, 191–204.
Shantser, A.E., Krayevaya, T.C., 1980. Formational sequences of subairial volcanic belt (on example of lake Cenozoic of Kamchatka) Moscow. Nauka publisher. in Russian.
Sheimovich, V.S., 1979. Ignimbrites of Kamchatka. Moscow, Nedra. 179 p.
Sheimovich, V.S., Karpenko, M.I., 1996. K–Ar volcanism of Southern Kamchatka. Volcanol. Seismol. 2, 86–90.
Sheimovich, V.S., Khatskin, S.V., 1996. Rhyodacitic magmatic formation of southeastern Kamchatka. Volcanol. Seismol. 5, 99–105.
Sheimovich, V.S., Golovin, D.I., 2003. Age of silicic volcanic rocks in the Bolshoy Banny springs. Volcanol. Seismol. 1, 21–25.
Schmitt, A.K., Grove, M., Harrison, T.M., Lovera, O., Hulen, J.B., Walters, M., 2003. The Geysers–Cobb mountain magma system California (Part 1): U–Pb zircon ages of volcanic rocks conditions of zircon crystallization and magma residence times. Geochim. Cosmochim. Acta 67, 3423–3442.
Simkin, T., Siebert, L., 1994. Volcanoes of the World, 2nd ed. Geoscience Press, Tuscon. 349 p.
Simon, J.I., Renne, P.R., Mundil, R., 2008. Implications of pre-eruptive magmatic histories of zircons for U–Pb geochronology of silicic extrusions. Earth Planet. Sci. Lett. 266, 182–194.
Slater, L., Jull, M., McKenzie, D., Grönvold, K., 1998. Deglaciation effects on mantle melting under Iceland: results from the northern volcanic zone. Earth Planet. Sci. Lett. 164, 151–164.
Taran, Y.A., 2009. Geochemistry of volcanic and hydrothermal fluids and volatile budget of the Kamchatka-Kuril subduction zone. Geochim. Cosmochim. Acta 73 (4), 1067–1094.
Volynets, O.N., 1994. Geochemical types, petrology and genesis of Late Cenozoic volcanic rocks from the Kurile–Kamchatka island–arc system. Int. Geol. Rev. 36/4, 373–405.
Volynets, O.N., Uspensky, V.S., Anoshin, G.N., Valov, M.G., Patoka, M.G., Puzankov, Yu.M., Ananiev, V.V., Shypitsyn, Yu.G., 1992. Geochemistry of Late Cenozoic basalts from East Kamcatka and implications for geodynamic evolution of magma generation. Volcanol. Seismol. 12 (5), 560–575.
Volynets, O.N., Ponomareva, V.V., Braitseva, O.A., Melekestsev, I.V., Chen, C.H., 1999. Holocene eruptive history of Ksudach volcanic massif, South Kamchatka: evolution of a large magmatic chamber. J. Volcanol. Geotherm. Res. 91, 23–42.
Wallman, P.C., Mahood, G.A., Pollard, D.D., 1988. Mechanical models for correlation of ring-fracture eruptions at Pantelleria, Strait of Sicily, with glacial sea-level drawdown. Bull. Volcanol. 50, 327–339.
Waythomas, C.F., Wallace, K.L., 2002. Flank collapse at Mount Wrangell, Alaska, recorded by volcanic mass-flow deposits in the Copper River lowland. Can. J. Earth Sci. 39, 1257–1279.